**REPUBLIC OF TURKEY**
**YILDIZ TECHNICAL UNIVERSITY**
**GRADUATE SCHOOL OF NATURAL AND APPLIED SCIENCES**

# SPECTRUM SENSING PERFORMANCE FOR COGNITIVE RADIO NETWORKS BASED GENERALIZED FREQUENCY DIVISION MULTIPLEXING MODULATION OVER FADING CHANNELS

**NIDAA ABD AL-QADEEM MOHAMMED AL-HASAANI**

**MSc. THESIS**
**DEPARTMENT OF ELECTRONIC AND COMMUNICATION ENGINEERING**
**PROGRAM OF COMMUNICATION ENGINEERING**

**ADVISOR**
**ASSIST. PROF. DR. AHMET SERBES**

**İSTANBUL, 2018**

**REPUBLIC OF TURKEY**

**YILDIZ TECHNICAL UNIVERSITY**

**GRADUATE SCHOOL OF NATURAL AND APPLIED SCIENCES**

# SPECTRUM SENSING PERFORMANCE FOR COGNITIVE RADIO NETWORKS BASED GENERALIZED FREQUENCY DIVISION MULTIPLEXING MODULATION OVER FADING CHANNELS

A thesis submitted by Nidaa ABD AL-QADEEM MOHAMMED AL-HASAANI in partial fulfillment of the requirements for the degree of **MASTER OF SCIENCE** is approved by the committee on 04.04.2018 in Department of Electronic and Communication Engineering, Communication Program.

**Thesis Adviser**

Assist Prof. Dr. Ahmet SERBES

Yıldız Technical University

**Approved By the Examining Committee**

Assist Prof. Dr. Ahmet SERBES

Yıldız Technical University _____

Assoc. Prof. Dr. Tansal GÜÇLÜOĞLU

Yıldız Technical University _____

Prof. Dr. Lütfiye DURAK ATA

İstanbul Technical University _____

## ACKNOWLEDGEMENTS

Foremost, I thank God for making everything possible to me.

I would like to express my heartfelt gratitude to my supervisor, Assist Prof. Dr. Ahmet Serbes for his guidance and assistance throughout the research. Furthermore, my appreciation goes to my beloved family (husband, mother, and brothers) for their love, sacrifices, encouragement, and moral support.

Additionally, I would like to express my deepest appreciation and thanks to the academic staff of Electronic and communication Engineering Department, Electrical and Electronics Engineering Faculty in Yıldız Technical University. Finally, yet importantly, I would like to thank all my friends, my classmates, and all of those who have helped me especially PhD student Ayhan Yenilmez.

April, 2018

Nidaa ABD AL-QADEEM MOHAMMED AL-HASAANI

## TABLE OF CONTENTS

Page

LIST OF SYMBOLS ..... vii

LIST OF ABBREVIATIONS ..... ix

LIST OF FIGURES ..... xi

LIST OF TABLES ..... xii

ABSTRACT ..... xiii

ÖZET ..... xv

CHAPTER 1

INTRODUCTION ..... 1

1.1 Literature Review ..... 4

1.1.1 Generalized Frequency Division Multiplexing ..... 4
1.1.2 Spectrum Sensing ..... 7
1.1.3 Spectrum Sensing with GFDM Background ..... 10

1.2 Objective of the Thesis ..... 12

1.3 Hypothesis ..... 12

CHAPTER 2

GENERAL INFORMATION ..... 14

2.1 Wireless Channels Models ..... 14

2.1.1 Additive White Gaussian Noise ..... 17
2.1.2 Rayleigh Fading ..... 18
2.1.3 Nakagami-n (Rician Multipath Fading) ..... 19
2.1.4 Nakagami-m Multipath Fading ..... 20

2.2 Filtered Multicarrier Systems ..... 21

2.2.1 Orthogonal Frequency Division Multiplexing (OFDM) ..... 23

2.2.2 Single Carrier with Frequency Domain Equalization (SC-FDE) ..... 26
2.2.3 Filter Bank Multicarrier (FBMC) ..... 28
2.2.4 Generalized Frequency Division Multiplexing..... 29

CHAPTER 3

MATERIAL AND METHODLOGY ..... 33

3.1 GFDM Transmitter ..... 34

3.1.1 GFDM Transmitter Model..... 34
3.1.2 Block Structure ..... 34
3.1.3 Baseband Modulator Processing..... 36
3.1.4 Generalized Frequency Division Multiplexing..... 37

3.2 Channel Model with Receiver Structure and Processing..... 38

3.3 Spectrum Sensing Using Energy Detection..... 40

3.4 Performance of GFDM with Energy Detection Based Spectrum Sensing ..... 41

CHAPTER 4

RESULTS AND DISCUSSIONS..... 44

CHAPTER 5

CONCLUSION AND FUTURE WORK ..... 51

5.1 Conclusions..... 51

5.2 Future work..... 52

REFERENCES ..... 53

CURRICULUM VITAE..... 52

## LIST OF SYMBOLS

| | |
|---|---|
| $T_{sym}$ | Symbol duration of a signal |
| $Bs$ | Signal bandwidth |
| $T_c$ | Coherence time |
| $B_c$ | Coherence bandwidth |
| $\alpha(t)$ | Rayleigh distributed for the channel |
| $h_l(t)$ | Path coefficient of the $l$-th tap at time $t$ |
| $x\,(t\,)$ | Discrete time input signal |
| $w(t)$ | Additive white Gaussian noise channel term |
| $y(t)$ | Additive white Gaussian noise channel term |
| A | Fading amplitude |
| $\mathrm{E_s}$ | Symbol energy |
| $N_0$ | Noise power density |
| $\boldsymbol{x}[n]$ | Transmitted signal |
| $\mu$ | Modulation order |
| $\vec{d}$ | Input data vector |
| $\vec{x}$ | Output samples |
| $K$ | Number of subcarriers |
| $M$ | Number of subsymbols |
| $F_s$ | GFDM sampled frequency |
| $T_s$ | GFDM sample duration |
| $F_{sc}$ | Spacing between adjasent subcarriers |
| $T_{sub}$ | Subsymbol duration |
| $T_b$ | Block duration |
| $d_{k,m}$ | Data symbol in $k$-th subcarrier and $m$-th subsymbol |
| $\boldsymbol{g}[n]$ | Prototype filter |
| $A$ | GFDM modulation matrix |
| $C$ | GFDM demodulation matrix |
| $\boldsymbol{r}[n]$ | Received data symbol |
| $\vec{\boldsymbol{H}}$ | Channel fading coefficients |
| $\lambda$ | Detection threshold |
| $m$ | Nakagami fading parameter |
| $H_0$ | Hypothesis test when there is no signal |
| $H_1$ | Hypothesis test when there is signal |
| $P_{fa}$ | Probability of false alarm |
| $P_d$ | Probability of detection |

| | |
|---|---|
| $P_{md}$ | Probability of missed detection |
| $N_p$ | Number of pilot symbols |
| $\boldsymbol{z}_p$ | Received pilot symbols after demodulation |
| $\boldsymbol{d}_p$ | Transmitted eceived pilot symbols after demodulation |
| T | Test statistic |
| $L$ | Number of blocks |
| $\vec{\boldsymbol{b}}$ | Input binary data |
| $N_{cp}$ | Length of cyclic prefix |
| $F_{\Delta}$ | Frequency gap |
| $\vec{\boldsymbol{x}}_{\boldsymbol{cp}}$ | Transmitted signal vector after adding cyclic prefix |
| iter | Number of Monte-Carlo realizations |
| No | Number of detected signals at the opportunistic user |

## LIST OF ABBREVIATIONS

| | |
|---|---|
| AWGN | Additive White Gaussian Noise |
| BER | Bit Error Rate |
| CAF | Cyclostationary Autocorrelation Function |
| CD | Cyclostationary Detector |
| CIR | Channel Impulse Response |
| CP | Cyclic Prefix |
| CR | Cognitive Radio |
| ED | Energy Detection |
| EGC | Equal Gain Combining |
| FBMC | Filter Bank Multi Carrier |
| FFT | Fast Fourier Transform |
| GFDM | Generalized Frequency Division Multiplexing |
| IAPFT | Interference Avoidance by Partitioned Frequency and Time Domain Transmission |
| ICI | Inter Carrier Interference |
| IFFT | Inverse Fast Fourier Transform |
| ISI | Inter Symbol Interference |
| LR | Likelihood Ratio |
| LOS | Line of sight |
| LS | Least Square Estimator |
| MMSE | Minimum Mean Square Error |
| MRC | Maximal Ratio Combining |
| MRT | Maximal Ratio Transmission |
| NEF | Noise Enhancement Factor |
| NP | Neyman–Pearson Test |
| OFDM | Orthogonal Frequency Division Multiplexing |
| OOB | Out-of-Band |
| PAPR | Peak Average Power Ratio |
| PBSK | Binary Phase-Shift Keying |
| PU | Primary User |
| QAM | Quadrature Amplitude Modulation |
| QoS | quality of Service |
| ROC | Receiver Operating Characteristic |
| RRC | Root Raised Cosine Filter |
| SC | Single Carrier |
| SC-FDE | Single Carrier- Frequency Domain Equalization |
| SC-FDM | Single Carrier-Frequency Division Multiplex |
| SER | Symbol Error Rate |

| | |
|---|---|
| SIC | Serial Inter-Carrier Interference Cancellation |
| SNR | Signal to Noise Ratio |
| SU | Secondary User |
| UFMC | Universal Filtered Multicarrier |
| ZF | Zero Forcing |

## LIST OF FIGURES

Page


Figure 1.1 Proposed (5G) application scenarios ..... 2
Figure 1.2 Measurement of 0-6 GHz spectrum utilization ..... 9
Figure 1.3 Overview for cognitive radio under hole spectrum concept ..... 10
Figure 2.1 Selected channel model block diagram ..... 16
Figure 2.2 Nakagami PDF for $\emptyset$ =1 with different values of the m fading parameter ..... 20
Figure 2.3 Example of FDM transmissions ..... 22
Figure 2.4 OFDM transceiver block digram ..... 24
Figure 2.5 SC-FDE transceiver block diagram ..... 26
Figure 2.6 SC-FDM transceiver block diagram ..... 27
Figure 2.7 FBMC/OQAM transceiver block diagram ..... 28
Figure 2.8 Complementary ROC curves for GFDM and OFDM ..... 30
Figure 2.9 Probability of missed detection, probability of false alarm versus different values of detection threshold ..... 30
Figure 2.10 Symbol error rate for GFDM transceiver over Nakagami-m fading channels ..... 31
Figure 3.1 Generic transmitter based GFDM ..... 34
Figure 3.2 Relevant variables and parameters in the context of GFDM ..... 35
Figure 3.3 GFDM modulation block ..... 36
Figure 3.4 Transmitter system model based on GFDM block ..... 38
Figure 3.5 GFDM receiver diagram ..... 39
Figure 3.6 Receiver model based on GFDM with energy detection blocks ..... 39
Figure 3.7 Standard energy detector block ..... 40
Figure 3.8 Simulation algorithm to calculate the $P_d$ ..... 42
Figure 4.1 $P_d$ versus SNR curves over Rayleigh fading channel at the receiver and after data equalization based GFDM ..... 45
Figure 4.2 $P_d$ versus SNR curves over Rayleigh fading channel at the receiver and after data equalization based OFDM ..... 45
Figure 4.3 $P_d$ versus SNR curves over Rayleigh fading channels for GFDM and OFDM after data equalization. ..... 46
Figure 4.4 $P_d$ versus SNR curves over Nakagami-m fading channel for OFDM and GFDM after data equalization ..... 47
Figure 4.5 $P_d$ versus SNR curves over fading channels after data equilization based GFDM ..... 48
Figure 4.6 $P_d$ versus SNR for different $P_{fa}$ values over Rayleigh fading channel after data equilization based GFDM ..... 48

## LIST OF TABLES

Page

Table 3.1 GFDM and OFDM simulation parameters …….....44

## ABSTRACT

# SPECTRUM SENSING PERFORMANCE FOR COGNITIVE RADIO NETWORKS BASED GENERALIZED FREQUENCY DIVISION MULTIPLEXING MODULATION OVER FADING CHANNELS

Nidaa ABD AL-QADEEM MOHAMMED AL-HASAANI

Department of Electronic and Communication Engineering

MSc. Thesis

Adviser: Assist. Prof. Dr. Ahmed SERBES

Generalized frequency division multiplexing (GFDM) is the generalized scheme for the OFDM, SC-FDE and SC-FDM, which adds configuration flexibility by covering all special cases. The data in the GFDM system are divided into data symbols, where each data symbol is represented by subcarriers and subsymbols. Each data symbol is modulated with a corresponding adjustable pulse shaping, giving the GFDM a flexibility property. The second property of GFDM is that it provides a low out-of-band emission. Flexibility property makes the GFDM an essential solution for many emerging applications of wireless communication networks, such as machine type communication (MTC), tactile Internet, and gigabit wireless connectivity applications for the proposed fifth generation (5G). Due to its low out-of-band property, it is more appropriate for the cognitive radio (CR) networks, compared to the OFDM, where the CR networks allows secondary users temporarily utilize the idle frequency band. This is achieved by spectrum sensing. Many techniques are used to sense the spectrum usage. The most widely used algorithm is the energy detection technique, due to its simple implementation.

In this study, spectrum sensing performance for the CR networks with GFDM modulation over Rayleigh and Nakagami-m fading channels are analyzed by performing appropriate computer simulations. Energy detection method is implemented for the GFDM system to improve the spectral utilization. The spectrum sensing performance is determined by the receiver operating characteristic (ROC) curves, which

are represented by probability of detection $P_d$ and probability of false alarm $P_{fa}$. ROC performance curves are provided to evaluate the performance of the proposed energy detection based spectrum sensing with GFDM transceiver over the mentioned fading channels.

The results of the study show that the probability of detection $P_d$ increases with the increasing signal to noise ratio SNR for all channels. The sensing performance enhances when the energy detection is implemented after the data equalization at receiver side. We provide our results for Rayleigh and Nakagami-m channels, where the simulation results show that the highest $P_d$ is obtained for higher Nakagami fading parameter-m. Also the sensing performance comparison based on modulation types (OFDM, GFDM) is done. The simulation results show that the $P_d$ for transceiver based GFDM is outperformed with that OFDM.

Key words: GFDM, OFDM, cognitive radio network, spectrum sensing, energy detection, ROC curves, Rayleigh and Nakagami fading channels.

# ÖZET

## GENELLEŞTIRILMIŞ FREKANS BÖLMELI ÇOĞULLAMA MODÜLASYONLU SÖNÜMLEMELİ KANALLARDA BİLİŞSEL RADYO AĞLARI İÇİN SPEKTRUM BELİRLEME PERFORMANSI

Nidaa ABD AL-QADEEM MOHAMMED AL-HASAANI

Endüstri Mühendisliği Anabilim Dalı

Yüksek Lisans Tezi

Tez Danışmanı: Öğretim Üyesi Dr. Ahmet SERBES

Genelleştirilmiş frekans bölmeli çoğullama (GFDM), tüm özel durumları kapsayarak konfigürasyon esnekliği sağlayan OFDM, SC-FDE ve SC-FDM için genelleştirilmiş şemadır. GFDM sistemindeki veriler, her bir sembolün alt taşıyıcılar ve alt semboller tarafından temsil edildiği veri sembollerine bölünür. Her bir veri sembolü, GFDM'ye bir esneklik özelliği vererek, karşılık gelen bir ayarlanabilir nabız şekillendirme ile modüle edilir. GFDM'nin ikinci özelliği, düşük bir bant dışı emisyon sağlamasıdır. Esneklik özelliği, GFDM'yi, bahsi geçen beşinci nesil (5G) için makine tipi iletişim (MTC), dokunsal İnternet ve gigabit kablosuz bağlantı uygulamaları gibi kablosuz iletişim ağlarının yeni ortaya çıkan uygulamaları için önemli bir çözüm haline getirmektedir. Düşük bant dışı özelliği nedeniyle, CR ağlarının ikincil kullanıcıların geçici olarak boşta kalma frekans bandını kullanmasına izin verdiği OFDM ile karşılaştırıldığında bilişsel radyo (CR) ağları için daha uygundur. Bu spektrum algılama ile elde edilir. Spektrum kullanımını algılamak için birçok teknik kullanılmaktadır. En yaygın olarak kullanılan algoritma, basit uygulaması nedeniyle enerji algılama tekniğidir.

Bu çalışmada, Rayleigh ve Nakagami-m sönümleme kanallarındaki GFDM modülasyonu ile CR ağları için spektrum algılama performansı bilgisayar simülasyonları yapılarak analiz edilmiştir. Spektral kullanımını geliştirmek için GFDM sistemi için enerji algılama yöntemi uygulanmaktadır. Spektrum algılama performansı, $P_d$ olasılığı ve yanlış alarm $P_{fa}$ olasılığı ile temsil edilen alıcı çalışma karakteristiği (ROC) eğrileri tarafından belirlenir. GFDM alıcı-vericisi ile önerilen enerji algılama tabanlı spektrumun performansının, bahsedilen sönümleme kanalları üzerinden değerlendirilmesi için ROC performans eğrileri sağlanmıştır.

Araştırmanın sonuçları, $P_d$ tespit etme olasılığının, tüm kanallar için artan sinyal gürültü oranı SNR ile arttığını göstermektedir. Algılama performansı, alıcı tarafında veri eşitlemesinden sonra enerji algılandığında uygulanır. Rayleigh ve Nakagami kanallarına ait sonuçlarımızı, simülasyon sonuçlarının, daha yüksek Nakagami sönümleme parametresi-m için elde edilen en yüksek $P_d$'nin elde edildiğini göstermektedir. Ayrıca modülasyon tiplerine (OFDM, GFDM) dayanan algılama performansı karşılaştırması yapılmıştır. Simülasyon sonuçları, alıcı-verici tabanlı GFDM için $P_d$'nin OFDM ile daha iyi performans gösterdiğini göstermektedir.

Anahtar Kelimeler: GFDM,OFDM bilişsel radyo ağı, spektrum algılama, enerji belirleme, ROC eğrileri, Rayleighve Nakagami sönümlemeli kanallar.

# CHAPTER 1

# INTRODUCTION

Mobile communication is one of the essential tools of modern society. In the 1980s 1G which was the first generation of cellular systems came into existence; it was based on analog voice transmission. Cellular networks have, since then, developed rapidly during the past few decades. Each step in the development has presented its own innovations. From the second generation (2G), digital modulation was implemented in all subsequent cellular systems. Digital modulation offered many advantages over earlier systems such as improved battery life for mobile equipment, higher system capacity, and enhanced quality of service (QoS). In addition, 2G was revolutionized with the introduction of short message service (SMS), allowing the people to communicate better. Introduction of third-generation (3G) cellular system enabled internet access from mobile devices and increased the data rates to be almost as much as the wired data rate at that time. Around the same time, smartphones with large storage and greater processing power were introduced in the market. These smartphones were equipped with a camera and high screen resolution and helped users transfer media contents from/to content providers. The requirement for a higher data rate by consumers led to a fourth generation (4G) LTE to emerge with the higher data transferring rate and higher throughput that is required by social networks. In LTE, for the first time, the multicarrier system technology based on orthogonal frequency division multiplexing (OFDM) was used. In other words, the physical layer of the LTE was achieved by application of OFDM. The gradual progress of the mobile network systems has been attributed to the ‘need for speed’ that has led to a higher spectral efficiency, higher data rate, and higher throughput. However, higher throughput alone will not be enough to overcome the challenges that are foreseen for the future fifth generation (5G) of cellular networks. In addition to higher spectral efficiency and higher data rate another

requirement is the physical layer flexibility that could be achieved only by employing the new multicarrier scheme, the generalized frequency division multiplexing (GFDM). GFDM adds many features that could help the new 5G cellular generation to be applied in more scenarios and applications. Some of them are mentioned ahead and also depicted in Fig. 1.1

- bitpipe communication requires fragmented spectrum with low out-of-band (OOB) to easily comply with cognitive radio (CR) technology [1].

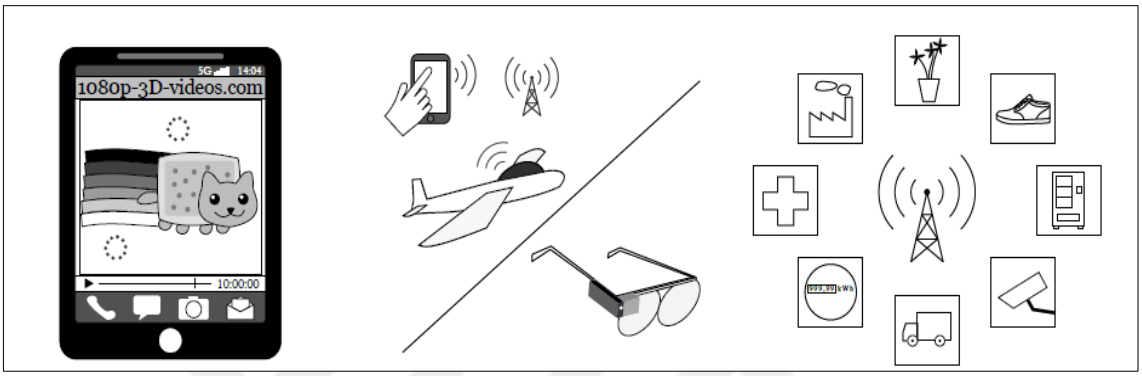


a) Bitpipe Communication b) Low- Latency Communication c) Machine Type Communication

Figure 1.1 Proposed (5G) application scenarios

- internet of things (IOT) requires devices to have battery support to connect them directly to the internet. Thus power consumption is a very important factor to take into consideration. IOT will serve as a large-scale sensor and mechanical operator. A huge collection of utilization cases can be abstracted by the term machine type communication [2]. This phenomenon can add reliable communications in exchange for a loose synchronization.

- tactile Internet / device-to-device communication scenario requires real-time control applications with round-trip latency at most 1 ms, for haptic, visual, and auditory interfaces. In general, ultra-low latency communication is determined by the physical layer, because less than hundreds of μs [3] of time is going to be a budget for the physical layer. The current LTE structure is based on 70 μs OFDM symbols which is considered as very high latency for tactile Internet. Therefore current LTE communication is not suitable for Tactile Internet.

- wireless regional area network scenario is usually implemented in licensed frequency bands. However, as they employ small cell stations, they may not be

as effective economically, especially in low populated areas. Due to the high emission generated by OFDM air interface causing a high OOB, it poses a challenge for spectrum regulations.

Based on the scenarios mentioned, the new next-generation network should achieve the following:

- large coverage areas, by using dynamic channel allocation based on CR.
- CR should be under low OOB emission conditions.
- low multipath effects on the overall data rate by decreasing the impact of the cyclic prefix (CP) insertion in the modulated data block.

In summary, the new next generation for a wireless network is urgently needed because of the new demands with more diversity of application requirements such as ultra-low latency, ultra-high data rate, some control applications that require a very short round-trip time, and battery-driven communication sensors which need ultra-low power consumption; OFDM is not able to serve these requirements. These reasons are enough for GFDM to take centrestage in development of a new network.

It is known that the licensed frequency band for the electromagnetic spectrum is almost completely assigned for various applications in wireless communications networks. The users of these applications call licensed primary users (PUs). Utilized frequency bands are dedicated to the licensed PUs who have the legacy rights and higher priority of services, based on television and radio broadcasting, cellular communications etc. which are governed by the regulatory bodies in the respective countries. Based on that, the licensed users need to pay fees to government offices such as the Telecom Regulatory Authority of India (TRAI) or Federal Communications Commission (FCC) in the USA for utilizing the frequency range. At the same time, the number of wireless devices and their users and the mobile networks and applications working on them have been dramatically increasing in recent years. Due to this scenario, the researchers have focused on radio spectrum optimization with the aim being utilization of the idle spectrum holes opportunistically for unlicensed secondary users (SUs) without causing harmful interference to the PUs. Additionally, it is indicated that the transient and geological varieties using the designated spectrum range from 15% to 85% [4]. Under these conditions, the idea of using CR is recommended by statutory enterprises like FCC, Office of Communications (Ofcom) in the United Kingdom, and standardization

groups like P1900, IEEE802.11af, and IEEE802.16h. CR allows the unlicensed SUs to access the licensed spectrum opportunistically when it is idle [5]. In order to mitigate the spectrum shortage with the condition that the incumbent PUs have to be protected from the interference generated by the opportunistic unlicensed SUs [6], [7], FCC has recently permitted unlicensed users to access the analog TV band [8]. The main objective of CR objectives is to enhance the spectrum efficiency while protecting the incumbent users from any unsafe interference. This can be achieved by spectrum-sensing techniques that play an essential role in CR. By matched filter detection [9], cyclostationary detection [10], energy detection [11], and last eigenvalue-based detection [12] techniques, spectrum sensing can be implemented. Every technique has its own calculations, advantages, and disadvantages. In our study, due to its low implementation and computational complexity, we chose energy detection techniques for spectrum sensing (it has also been covered and used in the literature review). Occupation of the specified frequency band by the PU leads to the presence of a certain energy level; otherwise, this frequency band may be available for an opportunistic user to use. Furthermore, the performance of the energy detection technique based on mainly spectrum sensing is determined by two parameters: the first one is the probability of false alarm and the second the detection probability. The probability of detection represents the presence of a PU signal in the specific frequency band. Detection probability also measures the interference level for the protection of incumbent users. Moreover, the probability of false alarm suggests that the opportunistic user has made a wrong decision about the occupation of the considered frequency band. As has been mentioned earlier, OOB emission that is generated from GFDM block is low; this makes the GFDM modulation an essential feature in CR, securing the incumbent user from any harmful interference that may be caused by opportunistic users.

## 1.1 Literature Review

### 1.1.1 Generalized Frequency Division Multiplexing

GFDM adds a flexibility property to the physical layer using non-orthogonality. This feature promotes GFDM as the leader for serving many new applications in wireless communication networks, similar to the newly proposed CR. GFDM provides low OOB radiation in CR networks. The flexibility feature costs GFDM by losing the subcarrier orthogonality, thus a high inter-carrier interference (ICI) is produced. ICI decreases the

GFDM performance. A significant number of studies have been done to enhance the GFDM performance and help it reach the OFDM performance in term of error rates. The traditional OFDM is limited with the rectangular pulse-shaped implementation that causes a high OOB radiation and is a good protector for ICI.

The first study on GFDM was done by Gerhard et al. in 2009 [13] which depended on the traditional filter bank approach for multi-carrier implementation. In their work, the GFDM basic concept was suggested and explained; they implemented the filter bank multi-branch digitally as a multicarrier scheme. Their studies have proved that a low peak average power ratio (PAPR) could be achieved by the application of GFDM. The studies further claimed that a reduction in power consumption and hardware cost is possible when implanting the GFDM transceiver concept as compared with the OFDM multicarrier block; this is an essential point of sale for future wireless systems. In addition, each subcarrier could have its own modulation (individually modulated) which gives it a high degree of flexibility in the system design. The GFDM bit error rate (BER) performance is seen to be not up to the mark because of the loss of the carrier's orthogonality. However, the GFDM BER performance can be controlled by choosing appropriate filter designs.

On the other hand, in 2011 Rohit et al. [14] focused on performance trends of GFDM. Their research studies the performance of many multicarrier concepts such as OFDM, filter bank multicarrier (FBMC), and GFDM. To enhance the FBMC performance, another equalization technique is added. This technique is applied per subcarrier and an associated feedback equalizer is employed for FBMC. The simulations show an improvement in the BER performance. Moreover, they have studied ICI cancellation for GFDM systems by adding a serial interference cancellation (SIC) for GFDM receiver block to enhance its performance. A simulation comparison in terms of BER performance was reported for GFDM with and without SIC effects.

Another work was presented by Rohit et al. [15] in 2012 which investigates the ICI cancellation for GFDM modulation technique. They have proved that the cancellation of the ICI leads to an improvement in BER performance for the GFDM technique. They used double-sided SIC with 3 iterations to cancel the ICI completely. Briefly, the interference could be cancelled for a specific subcarrier by usage of double-sided SIC. Its methodology depends on the estimation of the interference for the next subcarrier. Double-sided SIC can be defined as a hybrid between pure parallel and pure SIC

techniques.

However, Nicola et al. in 2012 [16] reported a linear system description for GFDM transmitter by arranging the data into time frequency. They took in consideration the GFDM system block description with the signal processing steps up-sampling, pulse shaping, up-conversion as matrix operations for both, the transmitter as well as the receiver. Three standard receivers (zero forcing (ZF), minimum mean square error (MMSE), and match filter (MF)) were used for signal detection. The BER performance was studied with analytical calculation and simulation. This study was applied for each receiver detection technique and for both CP-OFDM and the new GFDM blocks over additive Gaussian white noise (AWGN) and Rayleigh fading channels.

In 2015, Shravan et al. [17] analyzed the exact symbol error rates (SER) performance for GFDM transceiver over different fading channels such as Nakagami-m and Rician fading channels theoretically and compared it with the results that were obtained from a simulation. QAM mapping and ZF detection receiver have been derived from their work.

In 2015, Arman et. al. [18] examined how GFDM receiver could be designed with low complexity. They applied the discrete Fourier transform (DFT) to reduce the receiver complexity. The advantages of the demodulation matrix sparsification for this application have been utilized. They found a great reduction in complexity in the matrix multiplication and inversion operations that were achieved for the standard receivers MMSE, MF, and ZF criteria. This complexity reduction led to reducing the computational cost without any impairment in the system performance. They analyzed the computational cost of their proposed technique and got a lower computational cost for the MMSE and ZF receivers compared with that obtained by Ivan in 2013 [19] and one that was closer in complexity to OFDM receiver.

Hence, the OFDM modulation depends on the orthogonal characteristic that is worth the system protection from Inter Symbol Interference (ISI) and, with the addition of a CP, can reduce the impact of ICI, Sumarsana et al. [20] in 2016 have tried to investigate the impact of filters by employing many types of pulse shaping (a rectangular pulse in OFDM systems) to reduce the OOB, PAPR, and signal receiver performance. They have used raised cosine, root raised cosine (RRC), and Gaussian filter for their investigations. Better performance resulted in terms of roll-off factor (ROF) and

standard deviation.

In 2016, Ayhan et al. [21] worked to enhance the SER performance by deriving GFDM transceiver with different numbers of antennas. Antennas have been derived on the transmitter side and rely on maximal ratio transmission (MRT) technique over Nakagami-m (several Nakagami channel environments were considered). Symbol error rate SER was considered in terms performance analysis. Moreover, they studied the critical impact of the ROF of RRC filter on the error performance. They noticed that the SER increases when the ROF is increasing, due to the escalation in the noise enhancement factor of the employed ZF receiver.

### 1.1.2 Spectrum Sensing

Along with the proliferation of existing wireless communication services and emerging wireless applications that require high data rates, the demand for more bandwidth is quickly increasing [22]. The utilization of the spectrum varies from country to country. The usage of the spectrum is determined by analyzing the measurement-based control parameters such as temperature and energy characteristics. In the current buildings, a fixed frequency band is allocated for each new wireless application. Spectrum access requests have been dramatically increasing in the recent years. It is difficult to allocate the appropriate spectrum to be used for new wireless communication services and applications in the near future; thus, a shortage of information can be anticipated [23].

In spite of the fact that the frequency spectrum is statically assigned to many applications and services, studies show that the spectrum is not utilized widely for these applications and services at certain frequencies, time intervals, and locations. Latest and recent studies have been focused on a new generation technology for spectrum allocation. They are considered dynamic spectrum access methods instead of static spectrum methods for utilizing the frequency spectrum. From this point of view, the idea of the CR concept has been proposed. The main concept of the CR is monitoring the whole frequency band at a certain time and location while exploiting the idle spectrum in intelligent processing. As a result, the allocation of SUs can be useful and effective for the ability to eliminate the gaps in the white spectrum (idle frequencies) and cover the shortage of the frequency band caused by the licensing of PUs.

For instance, in 2007 Rakesh [23] conducted a study in the United States on the usage of spectrum in the 9 KHz to 1 GHz frequency band, and the spectral purity analyzed. In

this study, it was observed that usage of a large part of the frequency spectrum was somewhat rare.

The FCC have made the possibility of using the non-licensed SUs to occupy the licensed frequency band with dynamic distribution access for more efficient usage of trace resources. In 1999 Spectrum Sensing emerged for the first time. The CR term was proposed by Joseph and Gerald in order to increase the usage of the white spectrum [24]. A report was also produced on FCC's spectrum policies in 2002 [25]. The fundamental problem of the frequency domain is distribution as a constant in the frequency band. However, FCC's report draws attention to studies on technologies that suggest the usage of the frequency band dynamically instead of statically distributing so as to avoid the inefficient use of the frequency band. Several of these studies have been carried out within the Defense Advanced Research Projects Agency (DARPA) and the National Institute for Information and Communication Technology (NICT) as well.

Danijela et al. [26] have taken the critical wideband multi-gigahertz into consideration and used a matched filter, cyclostationary feature, and energy detection techniques. These techniques have been implemented to sense the environments in the spectrum. Also, they have checked the flexibility to adapt the transmission parameters in order to increase system capacity while co-existing with the incumbent users in the wireless networks. The power spectral density of the received signal with 6 GHz wide has been measured in downtown Berkeley. From Fig. 1.2 it is clear that the spectrum from 3-6 GHz had extremely low utilization; this supported the study conducted by FCC [4]. They observed that the advanced cyclostationary feature sensing was the best one in terms of its ability to differentiate modulated signals, interference with PUs, and noise in low SNR. Furthermore, it had more flexibility in transmission adaption sensing and was thus more efficient in cooperative systems.

Shibing et al. [27] have studied the collaborative spectrum sensing method in CR systems to improve spectrum sensing performance. Generally, in CR systems, the detection results by the SUs are sent to the fusion center (FC) through the reporting wireless channel to make the statistical test and provide the SU with the final decision. This reporting channel suffered from shadowing and fading effects in its practical usage. Due to this fact, collaborative spectrum sensing technology was proposed in their work. They tried to eliminate the shadowing effect of the reporting channel as much as possible by implementing the collaborative spectrum sensing technology. They applied

multihub diversity to transmit the detection result to the FC, whereby, they could reduce the BER.

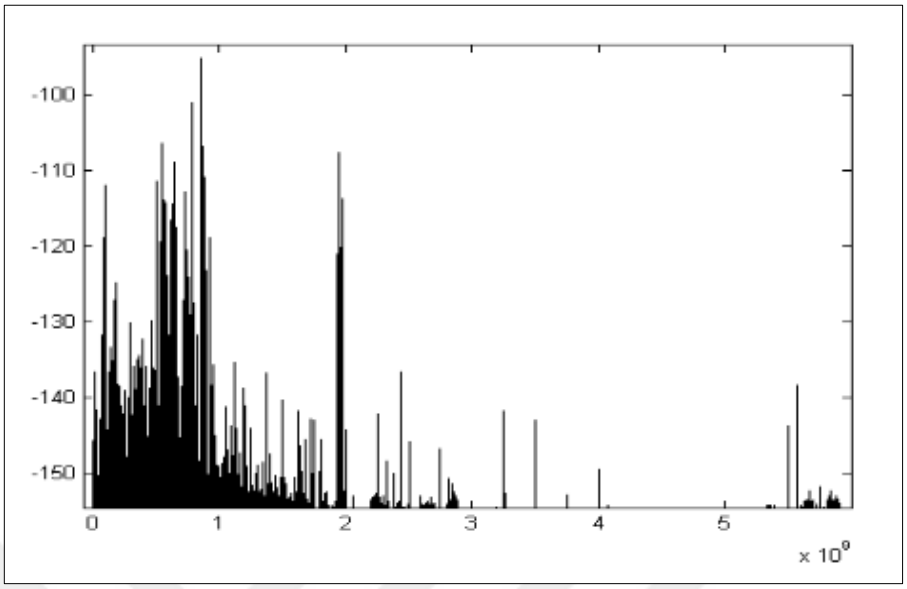


Figure 1.2 Measurement of 0-6 GHz spectrum utilization

Studies by Simon et al. [28] in 2009 solved the spectrum under-utilization problem in a computationally reliable and feasible manner. They detected the spectrum holes by spectrum sensing providing a high spectral-determination capability. The average power for each signal under specific sub-band was estimated and distinguished from any unknown directions of the interfering signals. Thus in this work, one of the essential requirements of CR communication, which is the process of perceiving the spectrum spaces (spectrum detection), has been provided.

Akyildiz et al. [29] have used the trace blanks as shown in Fig. 1.3. They have employed the spectrum detection algorithms as an effective and accurate method for detection of unoccupied channels. Haci's work in 2011 [30] also aimed to reduce the channel attenuation effects by using receiver antenna diversity techniques. Diversity could be obtained from more than one antenna use in the receiver side to improve the performance of the spectrum sensing, which is realized by the energy detection method. In other words, system performance can be improved by using several antennas in the receiver to detect the spectrum usage. Signals at the receiver antennas combine using techniques such as selective combining, maximum ratio combining, and equal gain combining. This means a low probability of error and a high probability of detection can be achieved in spectrum sensing. This performance improvement can be obtained by cooperation which can be augmented by using more than one antenna in the target

receiver and also by diversifying the receiver antenna.

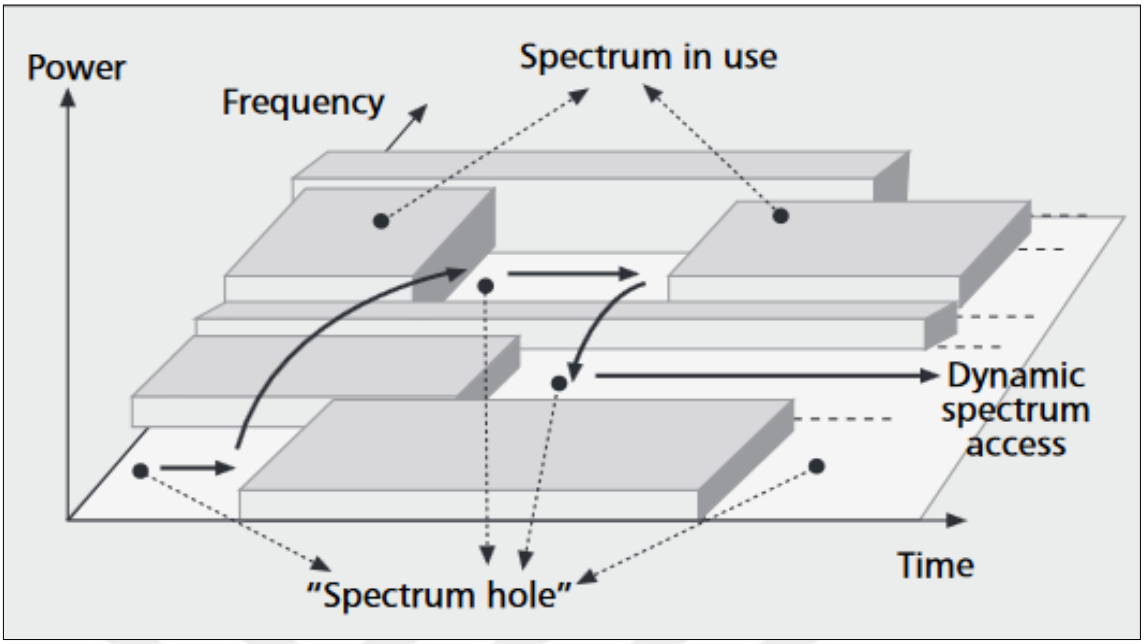


Figure 1.3 Overview for cognitive radio under hole spectrum concept

### 1. 1.3 Spectrum Sensing with GFDM Background

GFDM is a multicarrier physical layer, which it is suitable for CR networks due to its ultra-low OOB radiation feature. Any pulse shaping implements in GFDM transceivers give a good flexible physical layer property. These features of the GFDM promote it as opportunistic for the white space license spectrum with acceptable protection for PU signals from any harmful interferences at the chosen frequency band. GFDM uses features which are attractive in spectrum fragmentation. Spectrum fragmentation is a typical technical challenge for digital communication in CR networks in terms of exploiting the white space in licensed TV ultra-high frequency bands. OFDM with high PAPR and high OOB radiation features enable to cover spectrum fragmentation challenges in CR networks.

Nicola et al. [31] in 2011 suggested a common OFDM primary system to face two SU systems based on AWGN transmission channel, one with conventional OFDM, and the other with the GFDM scheme. Hence we have two primary systems both with OFDM, which are designed under the same parameter conditions, such as subcarrier space and sampling frequency, while ensuring that both systems are orthogonal. The GFDM signals generated by the secondary system are designed non-orthogonally with the primary OFDM signals. Hereby, the GFDM system needs more parameters to define

such as the roll-off filter, pulse shaping filter type, and filter. They have noticed less interference produced by GFDM secondary system to primary system than the asynchronous OFDM secondary system for high SNR over both channels that are mentioned.

Both types of research [32] and [33] have been interested in spectrum sensing based on cyclostationary autocorrelation function (CAF) scenario for GFDM system block. Rohit et al. [34] in 2012 claimed that the GFDM signals have a low OOB emission due to flexible pulse shaping implementations and that they also have an advent tail biting which adds to GFDM circular detection properties. This motivated them to deal with side peaks characteristics in CAF that were present with the GFDM signals, compared with the OFDM. They also analyzed the effect of the filter ROF on the detection result when the side peak CAF was used.

Dorin et al. [33] focused on cyclostationary detection (CD) properties for both OFDM and GFDM. With simulation, they proved that when the sum of all CPs was the same (circularity) for both GFDM and OFDM signals, similar CD performance resulted. But in case of low CP, the cyclostationary properties detected only the GFDM signal, indicating that GFDM was more reliable with smaller CP usage.

Rohit et al. [34] investigated in their research GFDM detection-based opportunistic users and the problem of spectrum sensing, regardless of the way of transmission, if there were no incumbent users in it. In other words, the opportunistic user senses the occupation of the channel by another opportunistic user. They assumed that the incumbent users were protected using the geo-location database concept. Hence their aim was to determine if the licensed TV white frequency band was occupied by any other cognitive user at any given time (GFDM-based opportunistic).

Intensive research has been done for OFDM-based spectrum sensing [35], [36], [37]. The studies have also extended to include the calculation of receiver sensing characteristics of the CR OFDM signal. Generally, they have depended on energy detection scenario for spectrum sensing. The probability of missing and probability of detection, the traditional parameters for characteristic sensing description for the OFDM opportunistic receiver, are derived mathematically. Rohit et al. [38] collaborated with another research team to examine this further to elaborate on their previous work. They have relied on the same idea to propose that the primary incumbent signal can be

secured with a geo-location database inquiry system. It is important for CR operation that OUs sense when operating in the same frequency band. They have presented a simulation study with its analysis to compare between the receiver operating characteristic (ROC) curves for GFDM and previous modulation OFDM over AWGN channel. A perfect synchronization with match filer receiver type based sensing characteristics have been assumed in the simulation, once with the proposed GFDM and then with traditional OFDM as an opportunistic signal. They obtained ROC curves for GFDM system that match the complementary ROC curves for traditional OFDM sensor and identical theoretical calculations.

## 1.2 Objective of the Thesis

- analysis and evaluation of the spectrum sensing performance of GFDM and OFDM based CR network over Rayleigh, and Nakagami-m fading channels.
- to improve the spectral utilization, the energy detection method for spectrum sensing is considered. The performance of the proposed simulation study is investigated and presented through ROC curves.
- validation of the recent multicarrier modulation technique GFDM for CR networks and pointing out the sensing performance over fading channels.

## 1.3 Hypothesis

Cognitive radio allows for the opportunistic users accessing the licensed frequency band to cover the demands for frequency band and increase the spectral efficiency. The well-known orthogonal frequency division multiplexing (OFDM) not satisfies the cognitive radio requirements due to it has high out-of-band emissions and low spectral efficiency. The new generalized frequency division multiplexing (GFDM) multicarrier modulation has low out-of-band emissions. This leads lower interference with primary users and better sensing performance. GFDM is employed in this work and the energy detector is positioned the after the equalized demodulated data.

# CHAPTER 2

# GENERAL INFORMATION

The first part of this chapter will discuss those wireless channels models that are supported with their own mathematical models. The second part of the chapter will cover

- general information about filtered multicarrier systems
- types of filtered multicarrier systems
- essential specifics and mathematical expression beyond each model
- the results of the latest studies related to generalized frequency division multiplexing (GFDM) error performance, and
- generalized spectrum sensing performance-based cognitive radio network over additive white Gaussian noise (AWGN) channel.

## 2.1 Wireless Channels Models

In order to investigate any communication system, it is important to produce or generate modelling for the transmission channel; this helps analyze the system easily especially when combined with the available analytical tools and through simulation. The wireless channel transmission between the transmitter and receiver can be defined in different ways [39]:

- physical modelling in term of electromagnetic waves
- input/output model of the wireless channel in terms of linear time-varying system, baseband equivalent model, and additive white noise
- time and frequency coherence in terms of Doppler spread with coherence time, and delay spread with coherence bandwidth, and
- last statistical channel models in terms of modelling philosophy and Rayleigh and Rician fading.

The AWGN channel is the most frequently assumed model of a transmission channel in digital communication theory as a function of input/output model. However, for some communication systems, the AWGN channel is not very accurate and is thus considered a poor model [39].

The fading channel is the one essential type of non-Gaussian channel that frequently occurs in practical scenarios. Fading is the time-varying behavior in received signal energy that takes place because the wireless channel picks up many multipath reflections during transmission. There are two essential types of defined fading for wireless channels, mentioned in literature in the field of communications: large-scale and small-scale fading.

Large-scale fading normally corresponds to

- the attenuation in the average power of the signal
- path loss due to moving to large areas
- existence of obstacles in the signal path
- position and distance between the transmitter and the receiver are the most effective large-scale fading.

The available statistics of large-scale fading arrived at through computing suggest an estimate of path loss as a function of distance. This is usually printed out in terms of a mean-path loss (*n*th-power law) and shadowing that represents the log-normally distributed changes around the mean of the signal. Hence it can be said that large-scale fading is a combination of shadowing loss and path-loss [39].

While small changes in the spatial separation between the transmitter and receiver cause dramatic variations in signal amplitude and phase, it is termed small-scale fading and is frequency dependent.

Rayleigh fading is a type of small-scale fading, suitable for scattering mechanisms where the number of reflectors is small. In Rayleigh fading, there is no line-of-sight (LOS) signal component [39]. In this type of fading, the probability density function (pdf) can be described as the envelope of the received signal statistically. The small-scale fading envelope can be described by a Rician pdf in the presence of predominant non-fading signal components. In other words, a large independent number of LOS propagation paths (often called *specular* paths) exist with known magnitude. However, all statistical models are dependent on the shaping of the power spectral densities for

additive white Gaussian random forms by either frequency-domain or time-domain filtering, whereas for the accurate models, the Gaussian processes are estimated by the superposition of limited appropriately chosen sinusoids.

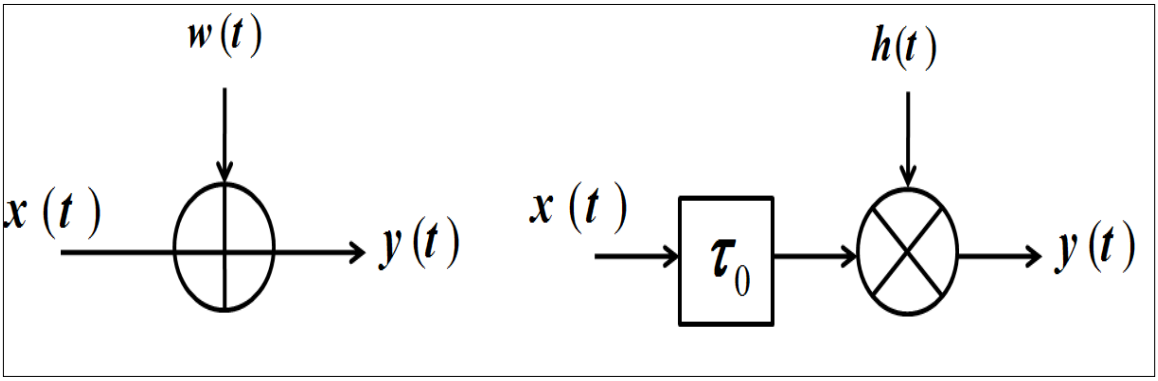


(a) AWGN (b) Rayleigh Fading

Figure 2.1 Selected channel model block diagram [40]

Accurate statistical models for fading channels are relayed on propagation properties and the underlying communication system. In our work, propagation properties are considered for the study while the antenna and circuits effects are disregarded. The most popular four wireless channel models: AWGN, Rayleigh, Nakagami-*m*, and Rician fading channels are briefly discussed ahead.

If a channel has a fixed response for a bandwidth more than the bandwidth of the transmitted signal, then such a channel is called flat-fading channel. The flat-fading channel and its conditions are expressed by [41]

$$T_{smy} \gg T_c$$
$$B_{smy} \ll B_c \quad (2.1)$$

where $T_{smy}$ and $B_{smy}$ are the symbols of the duration of a signal and signal bandwidth respectively, while $T_c$ is the coherence time over which channel coefficients are highly correlated and $B_c$ is the coherence bandwidth over which the channel coefficients are highly correlated. In the frequency domain, the flat-fading channel over the transmitted signal bandwidth has a fixed amplitude and linear phase response. So for this type of fading, the spectral characteristic of the transmitted signal is kept at the receiver. Hence, the channel impulse response (CIR) in a flat-fading channel can be written [41]

$$h(t) = \alpha(t)e^{-j\theta(t)} \quad (2.2)$$

where α(t) is Rayleigh distributed for the channel without an LOS path, it becomes Rician distributed in the presence of an LOS path with $\theta(t)$ uniformly distributed. A channel is defined by the frequency-selective channel when the signal bandwidth is more than the coherence channel bandwidth. For this particular case, different frequency components of the transmit signal undergo fading in varying degrees. So the conditions for a frequency-selective fading will be [41]

$$T_{smy} \ll T_c$$
$$B_{smy} \gg B_c \tag{2.3}$$

From the time domain impression, the symbol duration is less than the root mean square delay spread. The channel spreads the signal more than the symbol period and encourages generation of intersymbol interference (ISI) with the next transmitted symbol. Hence the frequency-selective fading channels can be expressed by

$$h(t,T) = \sum_{i=0}^{L_{t-1}} h_l(t)\delta(T - lT_s) \tag{2.4}$$

where $h_l(t)$ is the complex path coefficient of the $l$th tap at time $t$ whose amplitude is Rayleigh and phase is uniformly distributed.

Flat-fading channels are easier to model than frequency-selective fading ones because in frequency-selective fading each multipath signal is needed for modelling.

Since fading affects the narrow-band systems, the fading amplitude $\alpha$ modulates the received carrier amplitude, where $\alpha$ is a random variable (RV) with mean-square value $\Omega = \overline{\alpha^2}$, and the pdf $p_\alpha(\alpha)$ relies on the radio propagation properties or environment nature [42].

### 2.1.1 Additive White Gaussian Noise

Gaussian noise is the most common noise; the primary motivation behind the AWGN channel is to catch the noise from different sources like

- the thermal noise of components and circuits
- space radiation, and
- background noise or amplifier noise resources.

This noise leads to signal distortion that is not considered in the mathematical expression [42].

$$y(t) = x(t) + w(t) \tag{2.5}$$

Where $x(t)$ is the discrete time input signal, $y(t)$ is the output discrete signal for AWGN channel as given in figure 2.1(a), and $w(t)$ is the white additive noise channel term, that is expressed [40].

$$w(t) = w_{re}(t) + jw_{im}(t), w_{re}(t) \sim N\left(0, \frac{1}{2}\sigma^2\right), w_{im} \sim N\left(0, \frac{1}{2}\sigma^2\right) \tag{2.6}$$

This noise type consists of a complex RV with zero mean and variance $\sigma_w^2$ with Gaussian distribution for both, the real as well as the imaginary part. Subsequent realizations of noise are uncorrelated and are ordinarily assumed to be independent of the fading amplitude α statistically, which is considered to be a one-sided noise power spectral density $N_0$Watts/Hertz. Since the received instantaneous signal power is modulated by $\alpha^2$, then we can define the instantaneous signal-to- noise ratio (*SNR*) per symbol $\gamma = E_s/N_0$ multiplied by $\alpha^2$; hence, the average *SNR* per symbol becomes $\bar{\gamma} = \Omega\, E_s/N_0$ where $E_s$ is the symbol energy. Furthermore, the pdf of $\gamma$ that is determined in terms of pdf $P_\alpha(\alpha)$ fading pdf expression is [42].

$$p_\gamma(\gamma) = \frac{p_{\alpha\left(\sqrt{\frac{\Omega\gamma}{\bar{\gamma}}}\right)}}{2\sqrt{\frac{\gamma\bar{\gamma}}{\Omega}}} \tag{2.7}$$

The block diagram of the AWGN model is depicted in Figure 2.1(a).

### 2.1.2 Rayleigh Fading

Rayleigh Fading is a type of multipath propagation aspects. When the electromagnetic signal is scattered near to the receiver, the different paths can create delays under the resolution capabilities of the system. In that case, $\tau_0$is the signal delay assigned by all uncorrelated scatters. Moreover, all angles of arrival signals are equally assumed, and with the same average power received from each path is without line-of-sight connection. The all scatters superposition gives a time variant transmission, that is Rayleigh fading via equation 2.8, can be modeled as multiplication of the input channel with the random variable $h(t) = h_{re}(t) + jh_{im}(t)$. The channel output is given by [40]

$$y(t) = h(t)x(t-\tau_0), h_{re}(t) \sim N\left(0, \frac{1}{2}\sigma^2\right), h_{im} \sim N\left(0, \frac{1}{2}\sigma^2\right) \quad (2.8)$$

As a result, the phase of $h(t)$ follows a uniform distribution and $|h(t)|$ follows a Rayleigh distribution. The distribution of channel fading amplitude $\alpha$ can be represented as shown in Equation [42]:

$$p_\alpha(\alpha) = \frac{2\alpha}{\Omega} exp\left(-\frac{\alpha^2}{\Omega}\right), \quad \alpha \geq 0 \quad (2.9)$$

Usually, the performance is measured according to the *SNR* per symbol, so the instantaneous *SNR* per symbol under Rayleigh channel fading in terms of $\gamma$ distribution is expressed by [42].

$$P_\gamma(\gamma) = \frac{1}{\bar{\gamma}} \exp(-\frac{\gamma}{\bar{\gamma}}) \quad (2.10)$$

Rayleigh fading can be modeled as shown in figure 2.1(b).

### 2.1.3 Nakagami-$n$ (Rician Multipath Fading)

The Nakagami- $n$ distribution is also called Rice distribution [43]. It is a type of propagation path model that contains one strong direct LOS component with several random weaker components. Here the amplitude of channel fading follows the distribution as bellow, which is mentioned in [44, Eq. (50)]

$$p_\alpha(\alpha) = \frac{2(1+n^2)\, e^{-n^2}\alpha}{\Omega} \exp\left(-\frac{(1+n^2)\alpha^2}{\Omega}\right) I_0\left(2n\alpha\sqrt{\frac{1+n^2}{\Omega}}\right), \ \alpha \geq 0 \quad (2.11)$$

where $n$ is the Nakagami-n fading parameter with range from 0 to ∞. This parameter refers to the Rician $R$ factor, where $R = n^2$, which is compatible with the ratio of the power of LOS components to the average power of the scattered component. The SNR per symbol γ of the channel can be expressed by

$$P_\gamma(\gamma) = \frac{(1+n^2)\, e^{-n^2}}{\overline{\gamma}} \exp\left(-\frac{(1+n^2)\gamma}{\overline{\gamma}}\right) I_0\left(2n\sqrt{\frac{(1+n^2)\gamma}{\overline{\gamma}}}\right), \ \gamma \geq 0 \quad (2.12)$$

### 2.1.4 Nakagami-m Multipath Fading

Nakagami channels are used when the received signal has contributions from both diffuse and specular scattering, i.e., the electric field is the sum of a strong component (which is not necessarily LOS) and several contributions with less amplitude. The $m$ parameter relates the amplitudes of strong and weak components. The pdf for Nakagami multipath fading channel with channel gain α is produced by [44]

$$p_\alpha(\alpha) = 2\left(\frac{m}{\emptyset}\right)^m \frac{\alpha^{2m-1}}{\Gamma(m)} exp\left(-m\frac{\alpha^2}{\emptyset}\right), \quad \alpha \geq 0 \tag{2.13}$$

where $\emptyset = E(\alpha^2)$ is the average power for received signal, $\Gamma(.)$ is the gamma function [45], and $m$ is the Nakagami fading parameter ($m \geq 1/2$) The *SNR* $\gamma$ for symbol is employed according to the gamma distribution expressed by

$$P_\gamma(\gamma) = \left(\frac{m}{\bar{\gamma}}\right)^m \frac{\gamma^{m-1}}{\Gamma(m)} \exp\frac{-m\gamma}{\bar{\gamma}} \gamma \geq 0 \tag{2.14}$$

where $\bar{\gamma}$ is the average of the received *SNR*, while the phase of Nakagami fading is distributed uniformly over [0, $2\pi$]. Here the Nakagami fading multipath channel is introduced by a wide range via the $m$ fading parameter [46]. Hence the Nakagami-$m$ fading distribution represents the one-sided Gaussian distribution when $m$ =1/2 in the poorest fading case, while representing Rayleigh fading distribution for a special case when $m$ =1. The pdf of the Nakagami channel for different values of $m$ with fixed value of $\emptyset$ is shown in Figure 2.2 [42].

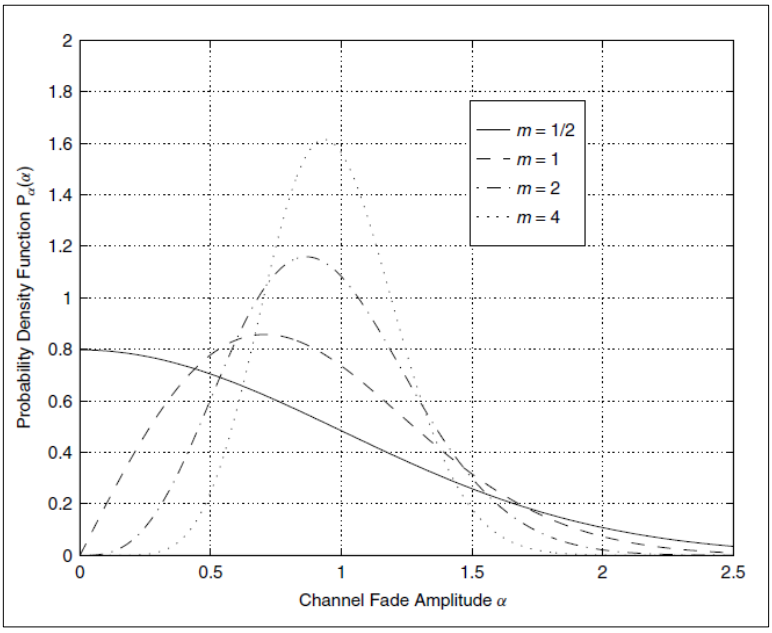


Figure 2.2 Nakagami PDF for $\emptyset$ = 1 with different values of the $m$ fading parameter

## 2.2 Filtered Multicarrier Systems

The first implementation of the multicarrier systems was in the 1950s in the field of military communications [47] while in the middle of 1960s, the concept of filtered multicarrier systems was deployed [48,49]. Orthogonal Frequency Division Multiplexing (OFDM) has appeared as the predominant waveform in communication systems [50].

The data information in multicarrier modulation system is divided into parallel streams and then transmitted over separate narrow-band sub-carriers, starting with a simple frequency division multiplex system (Figure 2.3). This frequency division in a frequency selective channel prevents the ISI if the sub-carriers have stretched a fraction of the channel's coherence bandwidth. This means a simpler equalization can be implemented once the fading effects per sub-carrier are considered flat fading. In addition, the multicarrier modulation is a good manager for spectrum resources and also shows fewer effects of interference that are caused by impulse noise [51]. The disadvantages of this scheme that limit its usage are

- high affectability to time changes of the fading channel during one symbol duration,
- a high peak-to-average power ratio (PAPR) [52] that causes strict linear power amplification with considerable output back-off.

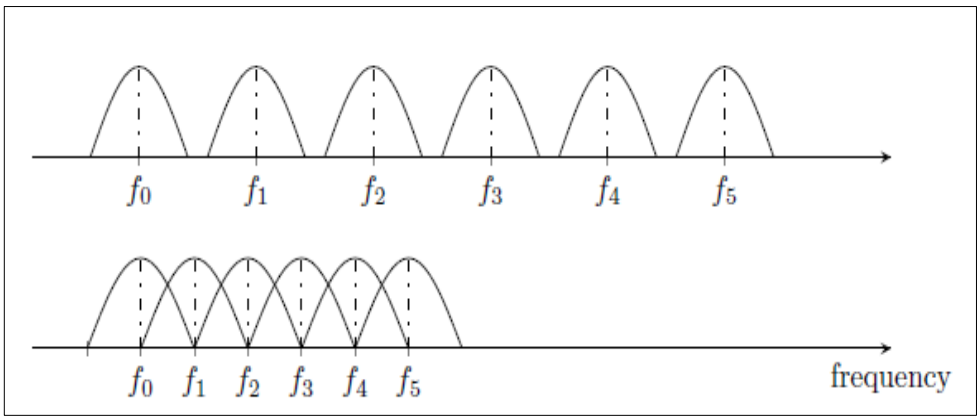


Figure 2.3 Example of FDM transmissions example

These days, OFDM is a common solution because it is an efficient FDM scheme with a robust performance in multipath channels. OFDM can use a cyclic prefix (CP) to get a cyclic convolution with the channel. Cyclic convolution helps to cancel the inter-carrier interference (ICI) and to perform a type of frequency domain equalization (FDE) by

implementing an efficient fast Fourier transform (FFT) algorithm. However, the application for these scenarios is expected to be utilized for next-generation 5G networks. The 5G networks present challenges for OFDM for its different single-carrier frequency domain equalization (SC-FDE) can only address the networks in a limited way [53], making it not the most promising required waveform for 5G. For instance, in OFDM, a rectangular window is used to shape every single sub-carrier in the time domain, while the resulting shape in the frequency domain for each sub-carrier is sinc-shape, leading to a non-negligible OOB. The leakage in OOB limits the OFDM implementation in fragmented spectrum applications or in the multiple access schemes with loose synchronization requirements. A lot of studies exist to find a solution to reduce OOB in OFDM. They are basically dependent on the bandpass filters that are put before transmission to achieve a required spectral mask. This solution has been successfully implemented in systems such as terrestrial integrated services, digital broadcasting, and terrestrial digital video broadcasting. They reach a critical mass with -50 dB spectral emission at only 5% surplus bandwidth [54]. In these two systems, a huge number of sub-carriers (in the thousands) and wide guard bands are used near the cut-off frequencies. In fact, even when the sub-carriers are in hundreds, it keeps from any significant degradation on the error ratio of filtered modulation.

Filter bank multicarrier (FBMC) method was posed as an alternative solution for OFDM where sub-carriers are pulse-shaped individually to eliminate the OOB emissions. The length of the impulse response for transmitting filter is often long and leads to a good spectral efficiency for continuous transmission [55]. This technique is able to serve applications that require a good fragmented spectrum, but it is poor for applications that require a low latency scenario with high efficiency in the short burst transmissions [56].

In the faster-than-Nyquist signaling (FTN) method, this can be introduced along with the FBMC concept. FTN is generated from overlapping of FBMC symbols along frequency axis [57] or the time axis [58]. This overlapping permits a higher transmission rate with the cost of self-interference (inter-carrier interference) and a substantially more complex receiver design [59].

In the universal filtered multicarrier scheme (UFMC), the impulse response length of the filter is reduced as continuous groups of sub-carriers are filtered to improve the OOB [60]. However, it does not consider the use of CP in FBMC, UFMC, and

straightforward FDE. This leads to it being incompatible with OFDM in performance and also making it more sensitive to small-time misalignment between users.

In the GFDM scheme, modulation is performed with block structure of a number of sub-symbols and sub-carriers [61]. A prototype filter is used to filtering the sub-carriers that are circularly shifted in the frequency and time domains; this filter can be designed to eliminate the OOB emissions and prevent a strong interference with incumbent users or other users of dynamic spectrum allocation and fragmented spectrum [62]. Moreover, SC-FDE and OFDM can be considered as special cases that, while retaining all main benefits, enable a new degree of freedom at the cost of additional implementation complexity. The next section will present more details about discussed waveforms and baseband models based on discrete time**.**

### 2.2.1 Orthogonal Frequency Division Multiplexing (OFDM)

A main advantage of OFDM is that it belongs to the multicarrier nature of this scheme. Here the wireless channel is divided into sub-channels in a multipath fading scenario [40]. If the bandwidth of the single sub-channels is less than the coherence bandwidth, then each sub-channel can be like a flat frequency. In combination with a cyclic prefix, the error rate is decreased; this allows simple channel equalization in the frequency domain by the zero-forcing receiver.

Orthogonality is making the symbols and sub-carriers independent of each other. By using the FFT algorithm, the OFDM block from the transmitter and receiver can be efficiently done in hardware. The disadvantage of OFDM is its high sensitivity to frequency offsets between transmitters and receivers, for instance those caused by

- doppler spread
- severe spectral leakage as well as unsuitable PAPR characteristics due to the nature of the signal multicarrier.

The basic block diagram of the OFDM transceiver is shown in Figure 2.4.

Let input data consist of complex-valued data symbols $\vec{d} = (d_n)$, where *n= 0,...., N-1*.

The transmit signal of OFDM can be represented as

$$x[n] = \sum_{k=0}^{K-1} g_k[n] d_k \qquad (2.15)$$

Where $n$ is the sample index in discrete time, $d_k$ is the OFDM data set symbol with $(k = 0,1, \dots, K-1)$, $g_k[n] = g[n].\exp\left[-j2\pi\frac{k}{K}n\right]$ is represents the subcarriers with the rectangular pulse shaping function

$$g[n] = \begin{cases} \frac{1}{\sqrt{K}} & for\ n = 0, \dots, K-1 \\ 0 & otherwise \end{cases} \quad (2.16)$$

The energy normalized to unitary, $\sum_{n=0}^{K-1} g[n]^2 = 1$.

The OFDM modulation signal can be represented compactly by using the matrix structure given as

$$\vec{X} = W_K^H \vec{\mathrm{d}}. \quad (2.17)$$

where $d = (d_k)$ and $W_K^H = (g_0 \dots . g_{K-1})$ consisting of the rectangular impulse responses of OFDM sub-carriers which are defined as column vectors, $g_k = (g_k[n])^T$ and as $W_K = \frac{1}{\sqrt{K}}(w_{k1,k2})$, where $w_{k_1,k_2} = \exp(-\mathrm{j}2\pi k_1 k_2/K)$ and $k_1 k_2\, \epsilon\, \{0,1, \dots . , K-1\}$ is the discrete Fourier transform (DFT) matrix by $K \times K$. By this FFT algorithm, the OFDM modulation can be implemented efficiently [62, 63].

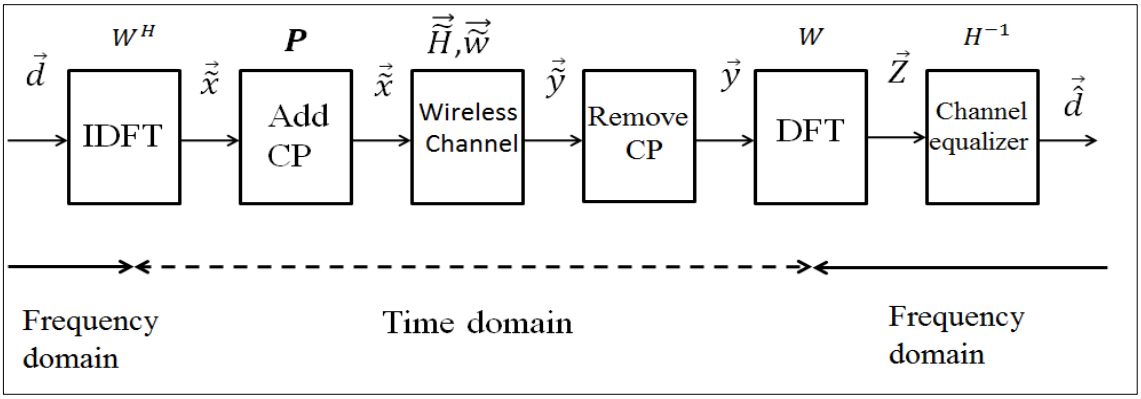


Figure 2. 4 OFDM transceiver block diagram

To avoid the ISI that is caused by multipath transmission affection in a wireless channel with channel length $N_{ch}$, added CP sample as a guard interval with length [64-66] $N_{cp} > N_{ch}$ allows for consecutive OFDM symbols to be processed without any interference. After addition of CP the transmitted signal given by

$$\tilde{\boldsymbol{x}} = \left[[x(-NCP)\ mod\ K] \cdots x[0] \cdots x[K\ -\ 1]\right]^T. \quad (2.18)$$

The operator $(\cdot)\ mod\ K$ denotes the remainder modulo $K$. But here the addition of CP reduces the spectral efficiency of the modulation system by a factor $\frac{K}{K+N_{cp}}$. The received signal for OFDM through wireless channel is represented by

$$\vec{\boldsymbol{y}} = \widetilde{\boldsymbol{H}}\vec{\boldsymbol{x}} + \vec{\boldsymbol{w}} \tag{2.19}$$

where $\widetilde{\boldsymbol{H}}$ is the channel matrix, which is a convolution matrix $\left(K + N_{cp} + N_{ch}\right) \times \left(K + N_{cp}\right)$ with band-diagonal structure [67] based on a CIR $= (h_0, \dots, h_{Nch-1})^T$, while $w \sim CN\left(0, \sigma_w^2 I_{K+N_{cp}+N_{ch-1}}\right)$ denotes noise with zero mean and various $\sigma_w^2$ that represent AWGN.

At the receiver, remove the CP under the assumption of perfect time and frequency synchronization and the channel being constant within the OFDM symbol duration, hence replacing $\widetilde{\boldsymbol{H}}$ with the $K \times K$ by matrix $\boldsymbol{H}$, the corresponding circular convolution matrix. In the receiver, the received OFDM symbol depends on the type of receiver, for instance, zero-forcing (ZF) receiver demodulation, so the channel equalization will be [50]

$$\vec{\boldsymbol{z}} = \mathbf{H}^{-1}\vec{\mathbf{y}}, \tag{2.20}$$

if *h* is available at the receiver and the estimated data symbol can be obtained with the help of DFT operation as

$$\vec{\widetilde{\boldsymbol{d}}} = \boldsymbol{W}_{\boldsymbol{K}}\vec{\boldsymbol{z}} \tag{2.21}$$

Data symbol can be obtained without matrix inversion, as a special case of ZF equalization, and benefit from the presence of the circulant channel matrix *H* [50] which is diagonalized by the DFT as

$$\boldsymbol{H} = \boldsymbol{W}_{\boldsymbol{K}}^{\boldsymbol{H}}\boldsymbol{\Lambda}\boldsymbol{W}_{\boldsymbol{N}}, \quad \boldsymbol{\Lambda} = \text{diag}(\boldsymbol{W}_{\boldsymbol{K}}\vec{\boldsymbol{h}}) \tag{2.22}$$

where $\text{diag}(\cdot)$ is the matrix it is diagonal with vector $(\cdot)$ and zeros for elsewhere. To obtain the estimation data symbols via fallowing equation, the equalization process needs to be combined with demodulation

$$\vec{\widetilde{\boldsymbol{d}}} = [\text{diag}(\boldsymbol{W}_{\boldsymbol{K}}\vec{\boldsymbol{h}})]^{-1}\boldsymbol{W}_{\boldsymbol{K}}\vec{\boldsymbol{y}} \tag{2.23}$$

Here the channel matrix with special structure and the inversion diag$(\boldsymbol{W}\vec{\boldsymbol{h}})$ require multiplication with a single coefficient for each data symbol.

### 2.2.2 Single-Carrier with Frequency Domain Equalization (SC-FDE)

In OFDM system, it is the symbol from the summation of a large number of independent sub-carriers; this made the system obtain a high PAPR property when compared with single-carrier systems [68]. High PAPR degraded the *SNR* of the analog-to-digital (A/D) and digital-noise-ratio (D/A) conversions. PAPR leads to reduction in the power-amplifier efficiency in the transmitter. This issue is a critical point for uplink direction because the battery power in a mobile terminal is limited.

The SC-FDE modulation scheme is sometimes referred to as 'precoded OFDM', but with an essential difference. Here the data symbols are described in the time domain rather than frequency domain [40]. Accordingly, the data in the OFDM symbol is allocated to a small bandwidth (sub-carrier) with long time duration, while in SC-FDE it is allocated to a whole bandwidth with short duration, which is relevant when using different channel models. This scheme is very useful for cellular uplink transmission because it offers a significantly better PAPR characteristic, as compared with OFDM. Besides, SC-FDE allows for part of the computational complexity to be shifted from the transmitter to the receiver.

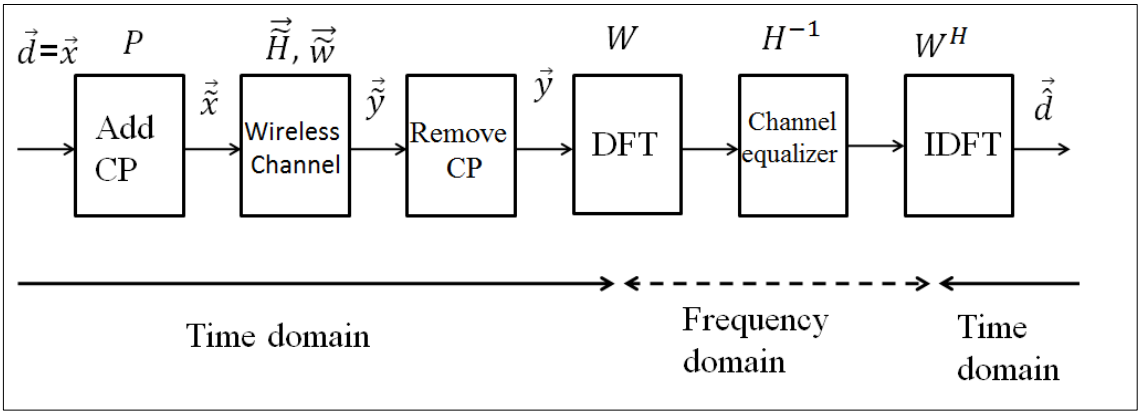


Figure 2.5 SC-FDE transceiver block diagram

A block diagram of the SC-FDE transceiver is presented in Figure 2.5. The transmitted symbols in SC-FDE can be obtained by multiplying the transmit data vector $\vec{d}$ by a Fourier matrix $W_K$ that will cancel out the IDFT operation in the transmitter side and is shown in 2.12. So a trivial expression will get

$$\vec{x} = \boldsymbol{W_K^H}(\boldsymbol{W_K}\vec{d}) = \vec{d} \tag{2.24}$$

that to refer to the entire SC-FDE modulation process. Here we can determine the spectral properties of the signal by the transmit filter which is used for D/A conversion or from next radio frequency (RF) filtering. In SC-FDE, channel equalization is executed in the frequency domain by adding CP as it is done for OFDM. The transmission model and equalization process stay the same as given in 2.19 and 2.20. The estimated data from SC-FDE is given by

$$\vec{\tilde{d}} = \boldsymbol{W_K^H}[\mathrm{diag}(\boldsymbol{W_K}\vec{h})]^{-1}\boldsymbol{W_K}\vec{d} \tag{2.25}$$

When we have compared SC-FDE demodulator with the OFDM counterpart (2.23), it is apparent that the IDFT was saved in the SC-FDE transmitter side and was shifted to the receiver side.

In the last section, the generalization of the approach will be derived in the following chapter. Single carrier-frequency division multiplexing (SC-FDM) can be shown as a series of many SC-FDE carriers in frequency as illustrated in Figure 2.6, where the basic idea is to consider *K* of SC-FDE's signals adjacent in frequency. Each signal holds the data $\vec{\boldsymbol{d}}_{\boldsymbol{k}}$, where $k = 0, \cdots, K-1$ and by simple multiplication with a $\vec{w}_k = \exp\left(-j2\pi\frac{k}{Kn}\right)$ complex oscillation is mapped to a certain frequency resource, resulting

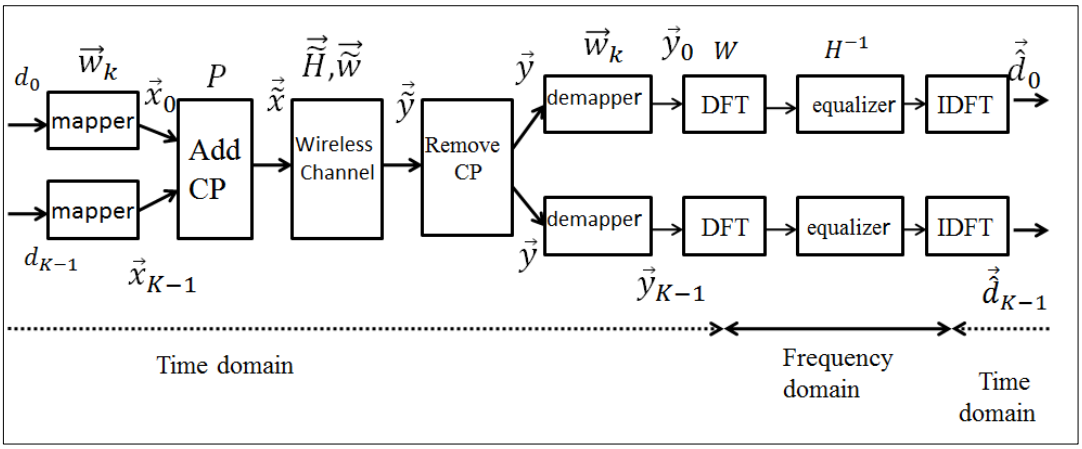


Figure 2.6 SC-FDM transceiver block diagram

in a waveform like individual sub-carriers in OFDM but with the difference that each carrier holds many data symbols. When many users are assigned to the carrier signal, the scheme is called single-carrier frequency division multiple access; this type of multiple access scheme is implemented in the uplink of long term evolution (LTE).

### 2.2.3 Filter Bank Multicarrier (FBMC)

The main idea in the filter that is extended is to cover multiple symbols with the ability to achieve a sufficient suppression of OOB emissions [69]. The filtering operation generates self-interference between symbols and sub-carriers. Self-interference is eliminated either by using only even or odd sub-carriers thus reducing the efficiency or by enabling real-orthogonality [70]. The real-orthogonality is obtained by

- separating the real part from the imaginary part of the data symbols
- modulating with an offset in time and frequency.

The offset quadrature amplitude modulation (OQAM) technique [70] is implemented in FBMC modulation. OQAM allows avoiding ISI and ICI. The FBMC/OQAM [71] system is shown in Figure 2.7. Consider $\vec{d}$ to be a dataset with a complex vector consisting of $N = KM$ QAM modulated data symbols and $\vec{q}$ its corresponding in OQAM modulated, where $K$ and $M$ are the number of sub-carriers and sub-symbols respectively in the system. Both vectors can be considered as a series of $K$ sub-carrier data vectors, that is, $\vec{d} = (\vec{d}_k^T)_{k=0,\dots,K-1}^T$ in the QAM formula and $\vec{q}=(\vec{q}_k^T)_{k=0,\dots,K-1}^T$ in the OQAM formula, hence the conversion from QAM to OQAM can be represented by

$$\vec{\boldsymbol{d}}_k = (\dots\ d_{k,m} d_{k,m+1} \dots) \tag{2.26}$$

$$\vec{\boldsymbol{q}}_k = \begin{cases} (\dots\ \mathcal{R}\{\boldsymbol{d}_{k,m}\} \quad \mathcal{I}\{\boldsymbol{d}_{k,m}\} \quad \mathcal{R}\{d_{k,m+1}\} \quad \mathcal{I}\{d_{k,m+1}\} \dots), & k \text{ even} \\ (\dots\ \mathcal{R}\{\boldsymbol{d}_{k,m}\} \quad \mathcal{I}\{\boldsymbol{d}_{k,m}\} \quad \mathcal{R}\{d_{k,m+1}\} \quad \mathcal{I}\{d_{k,m+1}\} \dots), & k \text{ odd} \end{cases}$$

which leads to double the number of elements and therefore the relative offset period between in-phase $(I)$ and quadrature-phase $(Q)$ is one half symbol [40]. In addition, there is a phase offset between the odd and even sub-carriers which causes $R(.)$ and $\mathcal{I}(.)$ alternate pattern. The $\vec{\boldsymbol{q}}$ vector is passed to the synthesis filter bank, which filters the data symbols on each sub-carrier. Based on low-pass prototype filter response, $\overrightarrow{\boldsymbol{g_s}}$ of each individual sub-carrier filter are with overlapping factor $L \times M$, which refers to sub-carrier length in sub-symbol duration. Then without adding the CP, the signal is transmitted through the wireless channel. On the receiver side, the analysis filter bank with prototype filter $\overrightarrow{\boldsymbol{g_a}}$ is used to receive the signal as is cleared in Figure 2.7. For each sub-carrier, the channel is equalized in time domain individually with a complex finite

impulse response filter based on a channel response $\vec{h}$ [72]. Finally, OQAM demodulates the symbol to obtain the received QAM symbol $\vec{\hat{d}}$.

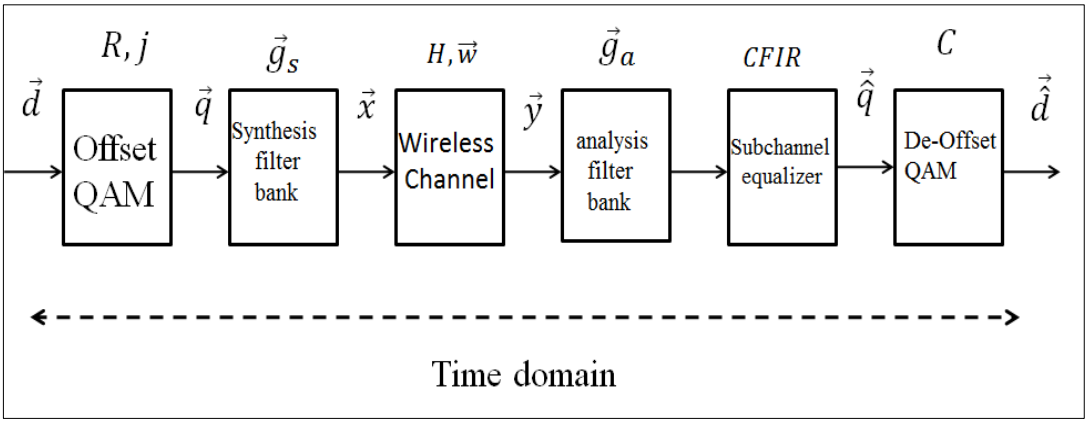


Figure 2.7 FBMC/OQAM transceiver block diagram

### 2.2.4 Generalized Frequency Division Multiplexing

GFDM is a filtered multicarrier modulation with block scheme which can transmit a block that consists of multiple sub-symbols per one sub-carrier [13, 61]. Circular pulse shaping is applied to each individual sub-carrier in GFDM. GFDM is also similar to the well-known OFDM system, with the selection of a rectangular pulse shape and single sub-symbol, and SC-FDE, when choosing a single sub-carrier with several sub-symbols. In GFDM each sub-carrier is pulse-shaped with the adjustable pulse shaping filter; this enables GFDM support applications with low OOB emissions. Thus GFDM is more appropriate for the CR physical modulation scheme, for instance, and prevent strict interference in incumbent services or other users in the context of the fragmented spectrum and dynamic spectrum allocation. This is clear from the simulation result obtained by Rohit et al. [38]. They have considered GFDM and OFDM scenarios as an opportunistic signal for energy detection based spectrum sensing simulation under AWGN channel. It is observed that the probability of missed detection versus the probability of false alarm (complementary ROC) curves for GFDM is better than OFDM. This suggest that GFDM can sense better than OFDM in an asynchronous cognitive radio system as illustrated in simulation Figure 2.8. Also, this simulation results are supported by deriving the theoretical performance as evidenced. It is also clear that when using a GFDM receiver as a sensor the ROC characteristics of a traditional OFDM system are improved. These simulation studies show that GFDM is more suitable for cognitive radio PHY than conventional OFDM, not only because of

better spectral shaping but also because of better sensing characteristics. In the following chapter, details of the basic principles of GFDM will be provided.

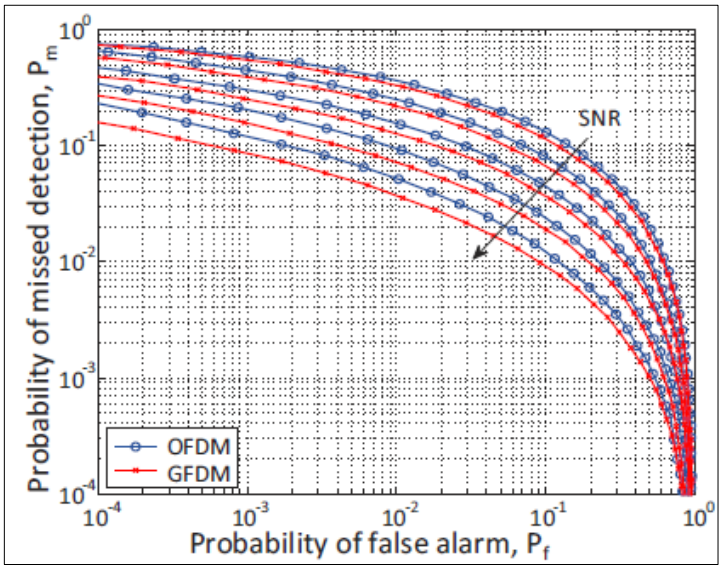


Figure 2.8 Complementary ROC curves for GFDM and OFDM with varying SNR

Rohit et al. [34] also focused on the probability of detection depending on the energy of the signal received for a cognitive radio system at a certain frequency. When the energy received was less than adjustable value it was termed detection threshold, indicating the

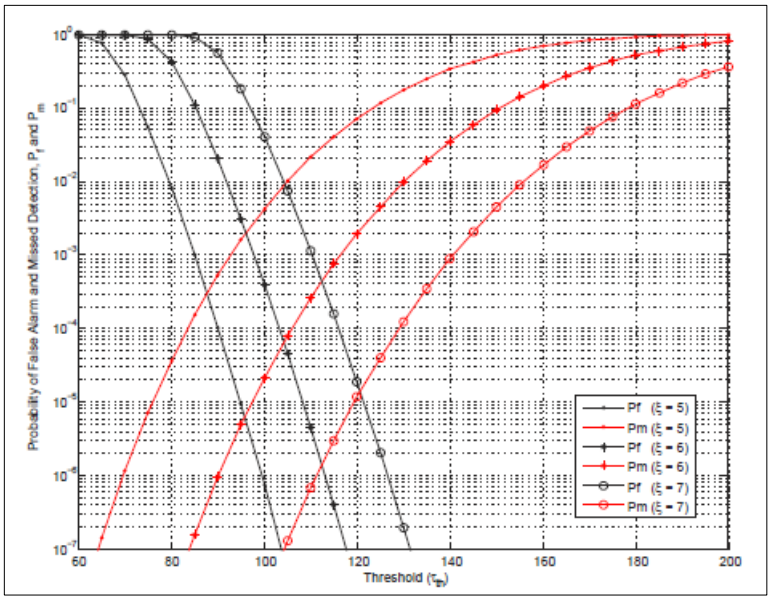


Figure 2.9 Probability of missed detection, probability of false alarm versus different values of detection thresholds

frequency is under null hypothesis ($H_0$) handled by noise power. If the power received was more than the threshold, this suggested that frequency for this instance is occupied by the incumbent or another opportunistic user and under alternate hypothesis ($H_1$).

According to this algorithm a spectrum sensing performance simulation was undertaken; one of them is depicted in Figure 2.9.

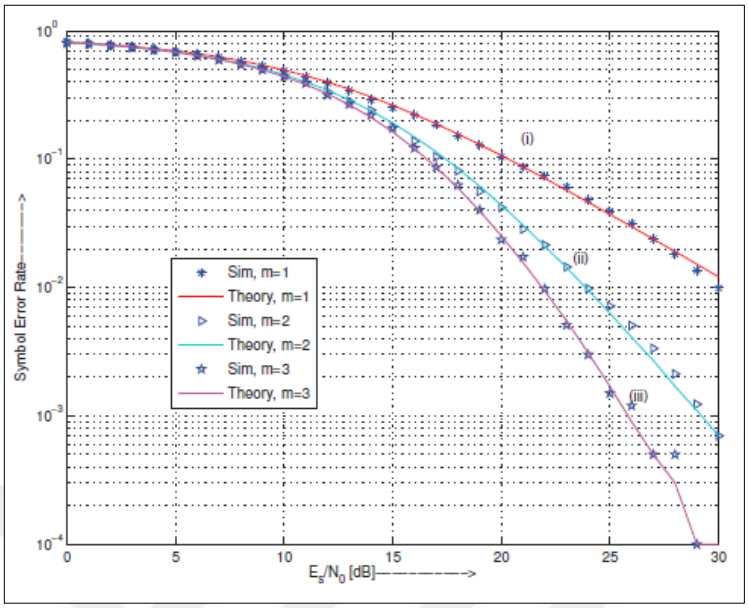


Figure 2.10 Symbol error rate for GFDM transceiver over Nakagami-*m* fading channels

Furthermore, the exact symbol error rate for GFDM transceiver under Nakagami-$m$ fading channels is illustrated in Figure 2.10 [17]. The lower error rate was achieved with the strongest fading channel $m = 3$, while highest error rate for $m = 1$ for Rayleigh is a special case of Nakagami-$m$.

# CHAPTER 3

# MATERIAL AND METHOD

## OVERVIEW

In previous chapter, the wireless channel models, and generic structure of filtered multicarrier systems for OFDM, SC-FDE, and FMBC have been explained. This chapter will present the sensing performance evaluation based on the cognitive radio system for GFDM, which form a basis for our research methodology. We are implementing an un-coded standard GFDM transceiver for sensing any user signal, incumbent or opportunistic. In addition, a basic zero forcing receiver with the least square estimator (LS) and an energy detection block are employed in order to sense the spectrum for GFDM signals. Details of GFDM signal generation and reception are illustrated. Moreover, the extensive simulation results will be presented and discussed thoroughly in order to evaluate the performance of the energy-detection-based spectrum sensing under Rayleigh and Nakagami-*m* fading channels in chapter four. This work can be considered as the extension of the initial work done by Rohit et al. [34, 38]. GFDM becomes the well-known OFDM system when using a rectangular pulse shape with single sub-symbol and it becomes the SC-FDE by applying a single subcarrier with many sub-symbols. The circularity principle allows GFDM to generate cyclic prefix (CP) and implement FDE to handle multipath effects in FSC. Hence GFDM is a generalized scheme for OFDM, SC-FDE and SC-FDM. Since the GFDM is the generalized case, it adds configuration flexibility by covering all special cases. Furthermore GFDM can be designed to eliminate the OOB emissions by using any pulse shape for each element, For instance, GFDM can be configured to avoid strict interference in incumbent services or other users in the context of the fragmented spectrum and dynamic spectrum allocation [73].

## 3.1 GFDM Transmitter

### 3.1.1 GFDM Transmitter Model

Figure 3.1 shows the generic structure of a generic transmitter based GFDM [73]. The processing chain is started with the source providing the vector of binary data $\vec{\boldsymbol{b}}$, which is subsequently mapped by using, for example, quadrature amplitude modulation (QAM). This modulation maps the generated bits to the $2^{\mu}$ symbols with complex constellation, where $\mu$ is the mapper modulation order. The resultant vector forms a data block structure $\vec{\boldsymbol{d}}$ with $N$ elements. The baseband modulator block applies a pulse shape for each element of $\vec{\boldsymbol{d}}$ to generate $\vec{\boldsymbol{x}}$ as output samples. Finally, $\vec{\boldsymbol{x}}$ samples are extended with adding cyclic prefix (CP) by copying $N_{cp}$ samples from the end of $\vec{\boldsymbol{x}}$ to the beginning, which produces $\vec{\boldsymbol{x}}_{cp}$ . In the current work, the CP was added to the output modulated samples. In order to send this signal over the wireless communication channel, $\vec{x}_{cp}$ is sent to the digital-to-analog (D/A) converter.

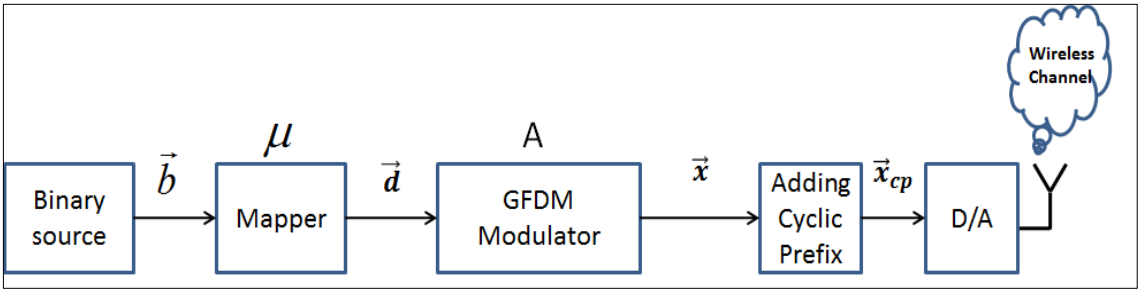


Figure 3.1 Generic transmitter based GFDM

### 3.1.2 Block Structure

The quantities block of transmitting and receiving data is a common approach in communication systems. In GFDM each block is assigned to hold $N = K \times M$ complex valued data symbols, which are distributed across $M$ sub-symbols and $K$ subcarriers. Figure 3.2 [73] displays an example for time-frequency grid, which is clarified with the terminology that will be used in our simulation. The data symbol is represented by the smallest unit in this block context. Each subcarrier contains $M$ data symbols which are transmitted respectively, which means using multiple time slots on a specific center frequency. In parallel, each sub-symbol represents $K$ data symbols that are transmitted in the same time slot using multiple center frequencies.

Based on the previous data block definition and assuming $F_s$ as a sampled frequency of

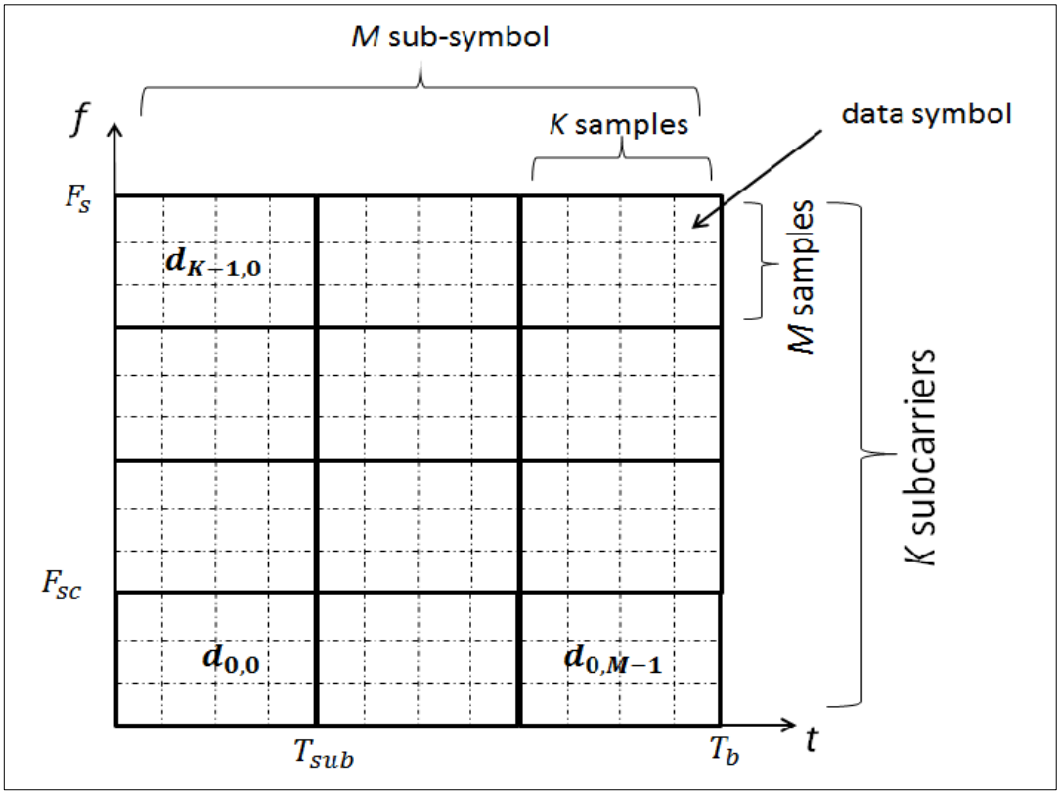


Figure 3.2 Relevant variables and parameters in the context of GFDM

the digital signal, the signal time and frequency dimensions can be calculated as fallows. First, the sampling duration is expressed via

$$T_s = \frac{1}{F_s}. \tag{3.1}$$

Since there are $K$ subcarriers in the system, the spacing between these subcarriers $F_{sc}$ is calculated as

$$F_{sc} = \frac{F_s}{K} \tag{3.2}$$

where the above definition permits to support non-orthogonal and orthogonal configurations with GFDM. The subcarrier distance can be smaller if it is not required to have the orthogonality option. Furthermore, $F_{sc}$ is the distance between the subcarrier center frequencies and does not necessarily represent the actual bandwidth that is occupied by the subcarrier. The inverse of $F_{sc}$ represents the duration of a sub-symbol $T_{sub}$ as

$$T_{sub} = \frac{1}{F_{sc}} = KT_s \tag{3.3}$$

As previously established, there are $M$ sub-symbols in a block. Hence the total block duration $T_b$ sums up as

$$T_b = MT_{sub} = NT_s. \tag{3.4}$$

In the frequency domain, the frequency gap ($F_\Delta$) between two samples of the signal can be determined by

$$F_\Delta = \frac{1}{T_b} = \frac{F_{sc}}{M} \tag{3.5}$$

Note that each sub-symbol is represented by $K$ samples in the time domain and each subcarrier consists of $M$ samples in the frequency domain.

### 3.1.3 Baseband Modulator Processing

In this section, signal processing in the GFDM modulator is described. The main idea of GFDM modulation in filtering approach is that each data symbol is filtered individually with a certain pulse shape and then all signal parts are super-positioned to form the transmit samples.

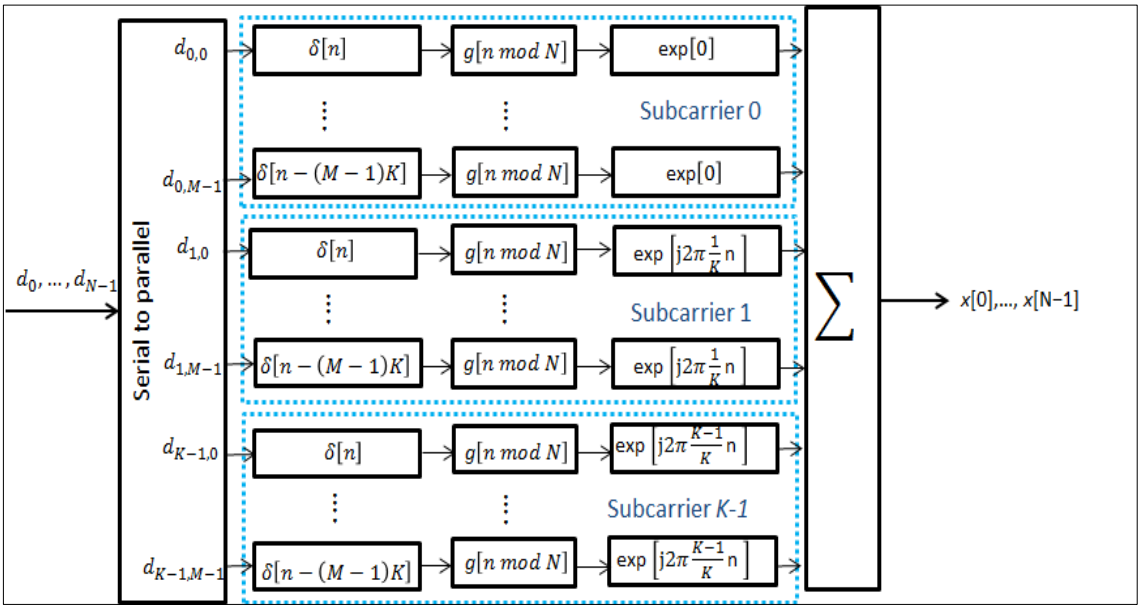


Figure 3.3 GFDM modulation block

It is shown in Fig. 3.3 [73] that the input data for GFDM modulation block contains $N$ elements with $d_n$ index. This symbol index is recomposed by serial to parallel block into $K$ subcarriers with $M$ sub-symbols, resulting a vector $\vec{\boldsymbol{D}}$, which denotes a data block

that contains $K$ subcarriers, $\boldsymbol{D} = [d_0^T, d_1^T, \ldots . d_{K-1}^T]^T$. Each subcarrier $d_k$ contains $M$ sub-symbols $\boldsymbol{d}_k = [\, d_{k,0}\, , d_{k,1}\, , \ldots . , d_{k,M-1}\, ]^T$, where $(\cdot)^{\mathrm{T}}$denotes the transpose. $d_{k,m}$ denotes the data symbol after QAM modulation transmitted on the $k$-th subcarrier and $m$-th sub-symbol in GFDM signal. The data vector after applying the serial to parallel converter can be defined by matrix form as

$$\mathbf{D} = \begin{bmatrix} \mathrm{d}_{0,0} & \cdots & \mathrm{d}_{0,\mathrm{M}-1} \\ \vdots & \ddots & \vdots \\ \mathrm{d}_{\mathrm{K}-1,0} & \cdots & \mathrm{d}_{\mathrm{K}-1,\mathrm{M}-1} \end{bmatrix}. \tag{3.6}$$

Hence, in the first step $N$ parallel elements from the signal path splitting are obtained, where $N = MK$ is assumed in our work. In each subcarrier, the related data symbol $d_{k,m}$ is multiplied by an impulse $\delta[n - mK]$, which has two impacts. First, each elements is up- sampled $K$ times, i.e., stuffed with $K - 1$ zeros. Here, to achieve for all subcarriers the Nyquist criterion in the system, it is necessary to put $KM \leq N$. Second, each data symbol is shifted in time domain by $mK$ samples, which moves sub-symbol position in the GFDM block. Next, each data symbol is circularly convolved with prototype filter $g[n]$, then is up-converted to its corresponding subcarrier frequency by inverse fast Fourier transform (IFFT) implementation. In other words, the data symbol is shifted in frequency domain [73]. Consequently, each data $d_{k,m}$ is modulated and transmitted with its own circular pulse shaping filter $g_{k,m}[n]$. It is necessary to note that the prototype pulse is defined with circularity $g[n] \equiv g[n \; mod \; MK]$.

Lastly, all elements of the signal are super-positioned to combine the transmit samples $\boldsymbol{x}$[n] with sample index $n = 0, \cdots, N - 1$. The result of the modulation can be expressed by

$$\boldsymbol{x}[n] = \sum_{k=0}^{K-1} \sum_{m=0}^{M-1} g_{k,m}[n] d_{k,m}\, , \mathrm{n} = 0,1,..N-1, \tag{3.7}$$

where $g_{k,m}[n]$ can represented by [74]

$$\boldsymbol{g}_{k,m}[n] = g[(n - mK) \bmod MK]. \exp\left[j2\pi \frac{k}{K} n\right]. \tag{3.8}$$

In a matter of fact, the circularity of pulse shaping adds tail biting property for GFDM signal [16], which helps to reduce the cyclic prefix (CP) needed. In other words, the transmitted signal can be expressed by a matrix structure given as

$$\vec{\boldsymbol{x}} = \boldsymbol{A}\,\vec{\boldsymbol{d}}. \tag{3.9}$$

where $\boldsymbol{A} = \left[g_{0,0}(n)^T g_{0,1}(n)^T \cdots g_{1,0}(n)^T \cdots g_{K-1,M-1}(n)^T\right]$ is the complex valued transmitter matrix with size of $MK \times MK$, consisting of prototype pulse shaping filters shifted in time and frequency domains, and $\vec{\boldsymbol{d}}$ is the transmit data vector. A cyclic prefix is appended with length $N_{cp}$ , hence the transmitted signal vector $\boldsymbol{x}_{cp}$ can be represented by

$$\vec{\boldsymbol{x}}_{cp} = \left[\boldsymbol{x}(MK - N_{cp} + 1 : MK); \boldsymbol{x}\right]. \tag{3.10}$$

Finally, it is sent to digital-to-analog (D/A) converter in order to send this signal over the wireless communication channel.

As a part of our simulation work, a prototype of square root raised cosine filter (RRC) has been implemented for impulse shape generation and the matrix **A** is composed. Each data symbol of $N$ elements is multiplied with it is corresponding pulse-shaping matrix **A**, that causes each subcarrier to shift in the frequency domain as result of the exponential multiplication. Moreover, each sub-symbol is also circularity shifted in the time domain. Consequently the transmitted GFDM signal is determined by (3.10). The GFDM transmitter system model based on this work can be alternatively summarized in Fig. 3.4 [38].

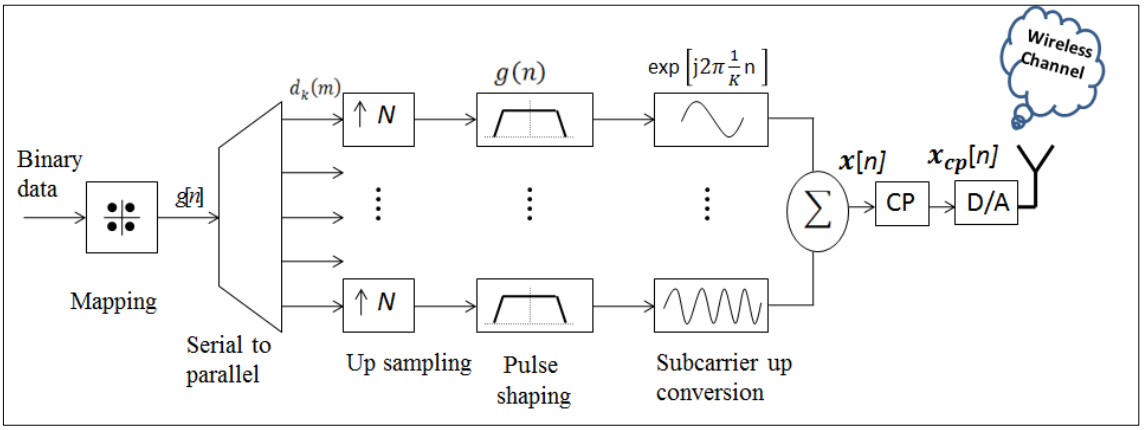


Figure 3.4 Transmitter system model based on GFDM block

### 3.2 Channel Model with Receiver Structure and Processing

The received signal $\boldsymbol{r}[n]$ at the receiver through wireless channel can be modeled by

$$\boldsymbol{r}[n] = \boldsymbol{H}\boldsymbol{x}[n] + \boldsymbol{w}[n] \tag{3.11}$$

when the CP effect is neglected

Here, $\boldsymbol{H}$ is the circular convolution matrix with size of $MK$ by $MK$ modeling the fading channel effect (channel fading coefficients matrix). In this work, multipath Rayleigh and Nakagami fading channels are considered, and we assumed the channel length is equal to 1. $\boldsymbol{w}[n]$ is the additive white Gaussian noise (AWGN) vector of length $N + N_{cp}$ with zero mean and variance $\sigma_w^2$. In addition, zero forcing receiver type has been used.

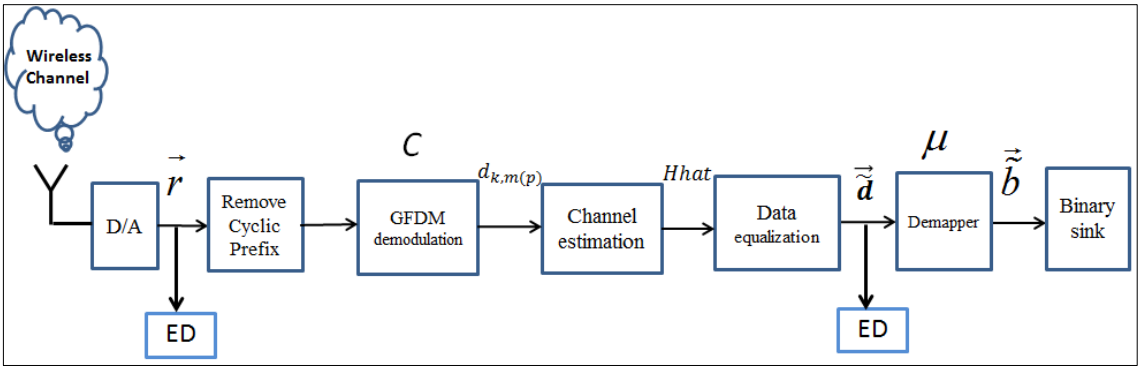


Figure 3.5 GFDM receiver diagram

In our work, the estimated data, which is obtained from the received data symbol $\boldsymbol{r}[n]$, is defined by [73].

$$\vec{\boldsymbol{D}} = \boldsymbol{C}\,\vec{\boldsymbol{r}} \tag{3.12}$$

where $\boldsymbol{C}$ is the demodulation matrix of GFDM, which is ideally selected as the matched filter receiver (MF), $\boldsymbol{C}_{MF} = \boldsymbol{A}^H$ [73].

The minimum mean square error receiver (MMSE), can be obtained by $\boldsymbol{C}_{MMSE} = (\boldsymbol{R}_n^2\,\boldsymbol{A}^H\boldsymbol{H}^H\boldsymbol{A}\boldsymbol{H})^{-1}\boldsymbol{A}^H\boldsymbol{H}^H$, where $\boldsymbol{H}$ is the channel matrix, $(\cdot)^H$ is the Hermitian operator, and $\boldsymbol{R}_n$ refers to the covariance matrix of the noise.

Last zero forcing receiver (ZF), is given by $\boldsymbol{C}_{zF} = \boldsymbol{A}^{-1}$. ZF is implemented in this work, which helps remove all self-interferences [21]. The receiver system model is illustrated in Fig 3.5 [74].

A pilot GFDM symbols $d_p$ are used as training symbols for channel estimation purpose. These symbols are sent uniformly in frequency domain after QAM mapper and before the GFDM modulation in transmitter side. 16 pilot symbols are sent in this work. The channel impulse response (CIR) is estimated in frequency domain. These references

pilot symbols are compared with that received pilot data information ($\boldsymbol{z}_p$) after the GFDM or OFDM demodulation. In this work the least square (LS) estimator has been employed for computing the estimated CIR. The estimated CIR of pilot symbols for LS estimator is given as [74]

$$\widehat{\boldsymbol{H}}_{\boldsymbol{p}} = \boldsymbol{d}_p^{-1}\, \boldsymbol{z}_p = \left[\frac{z_p(0)}{d_p(0)}, \frac{z_p(1)}{d_p(1)}, \ldots . \frac{z_p(N_p-1)}{d_p(N_p-1)}\right], \tag{3.13}$$

where $N_p$ is the number of the pilot symbols. The estimated CIR ( $\widehat{\boldsymbol{H}}$ ) of data symbols $\boldsymbol{d}_z$ can be obtained by interpolating the estimated CIR of pilot symbols. Spline method is employed for interpolation process. Hence, the equalized estimated data symbols given by

$$\widehat{\boldsymbol{d}} = \frac{\boldsymbol{d}_z}{\widehat{\boldsymbol{H}}}, \tag{3.14}$$

then the equalized estimated data symbols are passed through the energy detector (ED) block as shown in figure 3.5 and figure 3.6. The receiver system model for cognitive radio based spectrum sensing is illustrated in figure 3.6. In this study; we have two cases are taken in simulation consideration depended on ED block position in receiver side. In the first the energy detector block is positioned at the receiver before demodulation and in the second case it is positioned after equalization and in this case with employing the channel estimation technique in case of fading channel (Rayleigh and Nakagami-$m$).

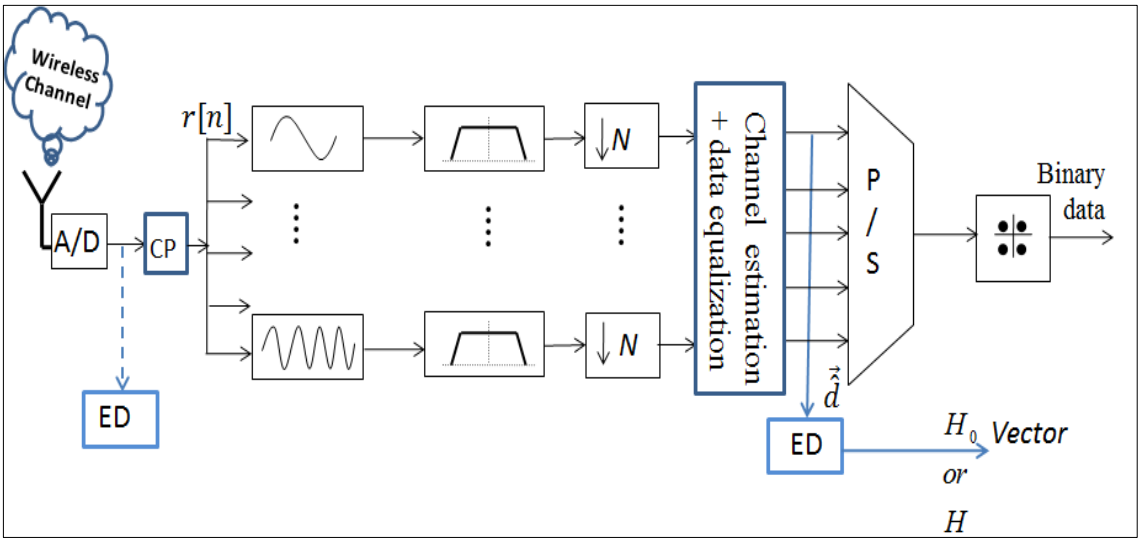


Figure 3.6 Receiver model based on GFDM with energy detection blocks

### 3.3 Energy Detection Based Spectrum Sensing with GFDM

The aim of spectrum sensing is to determine the absence of a primary user in the licensed frequency bands to allow the opportunistic user to utilize it. This has been done by implementing the energy detection block on the receiver side. In another words, spectrum sensing tests the white space for licensed bands if it is occupied by another cognitive user or not.

As a part of our work methodology, GFDM based opportunistic users are considered. The signal at the input of energy detector $\boldsymbol{r}[n]$ can be expressed by (3.15) with binary hypothesis testing problem. So, the received signal at opportunistic user, can be defined according to the binary hypothesis testing problem as

$$\mathbf{r} = \begin{cases} \boldsymbol{w} & ;\ H_0 \\ \boldsymbol{H}\,\boldsymbol{x} + \boldsymbol{w} & ;\ H_1 \end{cases}, \tag{3.15}$$

where $\boldsymbol{H}$ is the channel fading coefficient matrix, $\boldsymbol{x}$ is the transmitted GFDM signal and $\boldsymbol{w}$ is the AWGN vector.

The main approach for the Neyman–Pearson (NP) test is; the hypothesis test static defines as likelihood ratio (LR) is expressed by [76]

$$T_{LR} = \frac{p(r|H_1)}{p(r|H_0)} \tag{3.16}$$

where $p(.)$ represents the probability distribution function (pdf) under hypothesis $H_0$ and $H_1$ for the received signal at opportunistic users.

The test statistic under conventional energy detector implementation for multi-carriers is usually normalized according to the number of samples and the variance of noise that given by [76]

$$\mathrm{T} = \frac{1}{N\sigma_{\mathrm{w}}^2}\sum_{\mathrm{n}=1}^{N}|\boldsymbol{r}(\mathrm{n})|^2 \underset{\mathrm{H}_0}{\overset{\mathrm{H}_1}{\gtrless}} \lambda \tag{3.17}$$

The hypothesis $H_0$ is the decision for an opportunistic user depends on the detection threshold value λ, and indicates that the received signal at an opportunistic user is just only complex noise. In other words, the spectrum is not occupied by incumbent user (white space), and the opportunistic user can exploit this spectrum to transmit its signal. Contrarily, if the decision is based on the hypothesis $H_1$, it shows that the received

signal at an opportunistic is measured as an incumbent signal with noise and the frequency band busy with the primary or incumbent user.

### 3.4 Performance of GFDM with Energy Detection Based Spectrum Sensing

Here below are general terms that we need to highlight them as GFDM sensing performance evaluation:

The performance of spectrum sensing under energy detection algorithm is specified by probability of false alarm $P_{fa}$ and probability of detection $P_d$ [77]. Neyman-Pearson tried to increase $P_d$ for a target $P_{fa}$ which represented by ROC curve. $P_d = \text{Prob}\{ T > \lambda/H_1 \}$ represents the detection probability of a primary user signal in the specific frequency band, $P_d$ is a measure of the interference level, for the protection of the incumbent users. Low $P_d$ value results in absence of the primary user. Besides, the probability of missed detection is denoted by $P_{md} = 1 - P_d$. The probability of false alarm, $P_{fa} = \text{Prob}\{ T > \lambda/H_0 \}$ indicates that the opportunistic user is making wrong decision about occupation of the considered frequency band. The opportunistic user decides for a dedication of an incumbent user on the specified frequency, gives a decision with $H_1$, while the correct one is $H_0$. An increase in $P_{fa}$ results in low spectrum utilization by opportunistic users. So, for a better performance $P_{fa}$ should kept as little as possible [23, 24]. $P_{md}$ is the probability of miss detection means, which the percentage of frequency band that not occupied by incumbent users. According to Nayman-Pearson approach; for optimal detector design is to fixed one of these errors ( $P_{md}$, $P_{fa}$ ). In this approach fixed the $P_{fa}$ for a certain value and determine the $P_d$ accordinally [79].

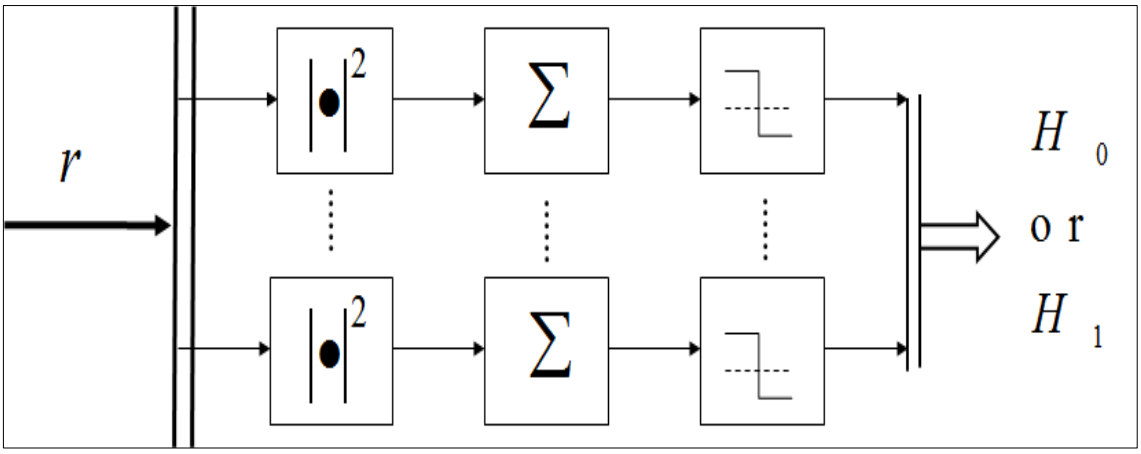


Figure 3.7 Standard energy detector block

In this research module, the $P_{fa}$ which is considered in this work is given by [78], [79]

$$P_{fa} = \mathrm{Q}\left(\frac{\lambda - L\sigma_w^2}{\sqrt{2L\sigma_w^4}}\right). \tag{3.18}$$

where $L$ is the number of GFDM block. The $\lambda$ is derived from $P_{fa}$ equation

$$Q^{-1}(P_{fa}) = \frac{\lambda}{\sqrt{2L\ \sigma_w^4}} - \frac{L\sigma_w^2}{\sqrt{2L\ \sigma_w^4}}$$

then at last the

$$\lambda = \sigma_w^2\sqrt{2L}\ Q^{-1}(P_{fa}) + \sigma_w^2 L\,. \tag{3.19}$$

Here, Here the threshold value is calculated according to the GFDM or OFDM L blocks at a required $P_{fa}$.

GFDM and OFDM simulation parameters are considered as in Tables 4.1 given in chapter 4. The standard energy detector block diagram as shown in fig.3.7 is considered, and ROC curves are obtained to evaluate the performance sensing with GFDM in cognitive radio networks.

Here, at the receiver for the opportunistic user; the received signal $\boldsymbol{r}[n]$ detects by the energy detector block as is shown in fig. 3.7. The square law device is applied to all samples in $\boldsymbol{r}[n]$, then the summing operation is implementing to get the energy of each GFDM or OFDM block. Hence, the test statistic $T$ can be is obtained by normalizing the energy of one block according to noise variance and number of samples as is written before in equation 3.17. Then comparing the test statistic $T$ with the detection threshold λ, which is illustrated and determined before in equation 3.19. If $T$ more than the threshold value λ means the detection detects an incumbent signal and the detection will decide that the frequency band is occupied by an incumbent user and considers under detection counter, if not the detection detects noise only and this frequency band is idle. This process is repeated for iter times (Monte-Carlo realizations). In this work the $P_d$ value is computed as average value according to L blocks.

As a summary, we simulated the $P_d$ for a given $P_{fa}$. The detection of an incumbent when the energy of pulse is more than or equal the detection threshold λ. We have simulated the $P_d$ at a certain value of $P_{fa}$ for different values of input SNR over

Rayleigh over Rayleigh, Nakagami- $m$ fading channels. The algorithm that used in MATLAB to simulate the performance of the energy detector for each block after data equalization is illustrated in figure 3.8. This algorithm is employed to simulate the $P_d$ depends on Monte-Carlo simulation. Where iter is the number of Monte-Carlo realization and No is the number of detected signals at the opportunistic user. Simulation results are obtained as it will be discussed in the following chapter.

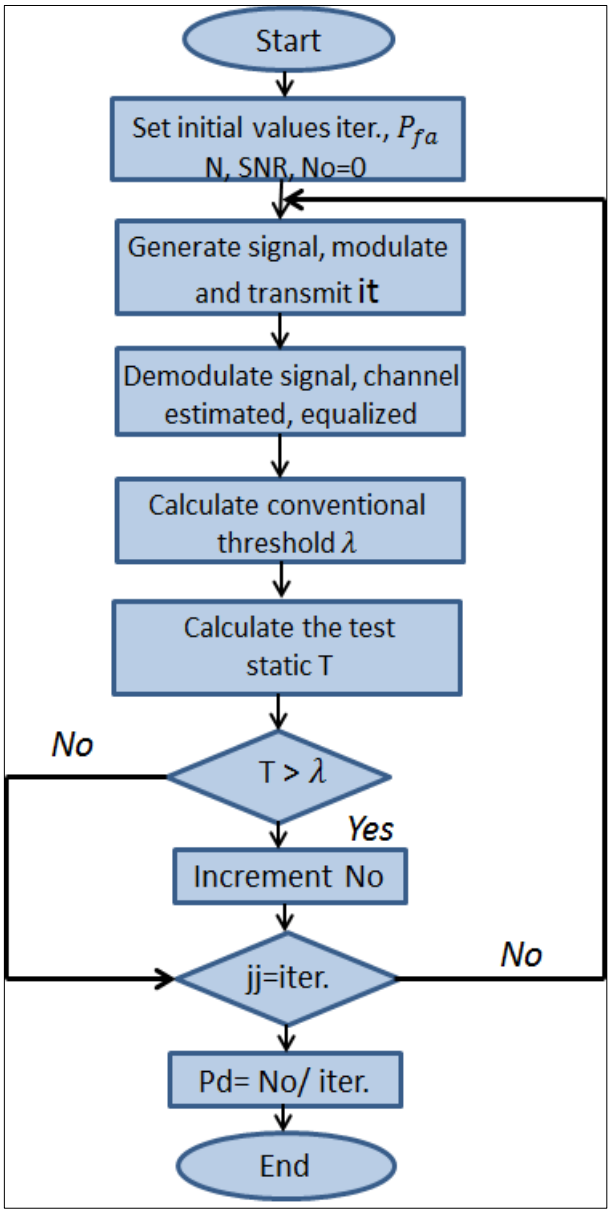


Figure 3.8 Simulation algorithm to calculate the $P_d$

Meanwhile, The ED is positioned once at the receiver directly after received the signal without any processing before, and the other after equalized the estimated demodulated

data as given in fig. 3.5. We have simulate the $P_d$ over a given SNR range for the two cases positions over Rayleigh and Nakagami-$m$ according to the above chart. The simulation results are given and explained in next chapter.

# CHAPTER 4

## RESULTS AND DISCUSSION

This study is focused on evaluating the performance of the energy detection based spectrum sensing method with GFDM multicarrier physical layer. The simulation parameters are set as in Table 4.1. where Rayleigh and Nakagami-*m* fading channels are implemented. Monte-Carlo simulation is employed with 1000 iterations.

Table 4.1 GFDM simulation parameters

| Parameter | Variable | GFDM | OFDM |
|---|---|---|---|
| Samples per symbol | $K$ | 64 | 64 |
| No. of subcarriers | $K$ | 64 | 64 |
| Block Length | $M$ | 5 | 1 |
| Number of block | $L$ | 20 | 20 |
| Filter type | $g[n]$ | RRC | rectangular |
| Roll-off factor | $\beta$ | 0.1 | - |
| Channels | $H[n]$ | Rayleigh, Nakagami-*m* | Rayleigh, Nakagami-*m* |
| Modulation | $\mu$ | 4/QAM | 4/QAM |

The spectrum sensing performance is evaluated by the probability of detection for a certain probability of false alarm according to the Neyman-Pearson theory. The probability of detection over Rayleigh fading and Nakagami-$m$ channels that are plotted

through ROC curves.

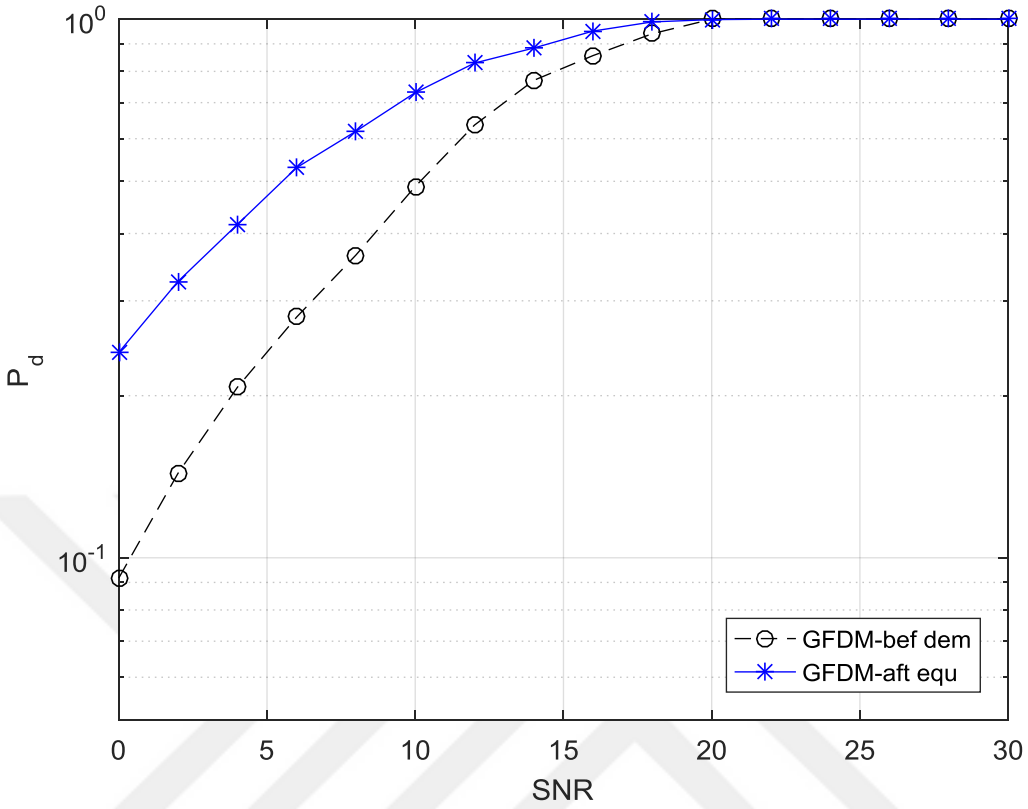


Figure 4.1 $P_d$ versus $SNR$ curves over Rayleigh fading channel befor the GFDM demodulation and after data equalization

The ROC performance curves for the spectrum sensing based GFDM and OFDM multicarrier physical layers over Rayleigh fading channel are illustrated in Figures 4.1, 4.2 respectively. The signal to noise ratio range from 0 dB to 30 dB and $P_{fa} = 10^{-3}$ are considered. For both, the simulation is done for the two positions, where the ED detects the signal before the demodulation and after the data equalization. In figure 4.1 the $P_d$= 0.2798 at SNR = 6 dB and 0.6359 at SNR= 12 dB in case of the energy detection before GFDM demodulation while equal to 0.532 at SNR=6 dB and 0.8289 at SNR=12 dB in case of the energy detection after data equalization. In figure 4.2 in case of the ED before the OFDM demodulation we get the $P_d$ is equal to 0.191 at SNR=6 dB and 0.4143 at SNR= 12 dB while when the ED is performed after the data equalization the $P_d$ is equal to 0.3685 at SNR=6 dB and 0.5793 at SNR= 12 dB. We can conclude two facts; once the probability of detection increases with increasing the SNR. The other fact; it is clear that the sensing performance for both after the data equalization

better than before modulation. Demodulation with equalization adds robustness for sensing performance by decreasing the noise and gives more pure signal.

While in Figure 4.3, a sensing performance comparison is illustrated, ROC bases on the demodulation types OFDM and GFDM are represented. The readings are taken after the data equalization for both GFDM and OFDM demodulation bases. For example the $P_d$ is equal 0.6194 at SNR = 8 dB and 0.8238 at SNR = 14 dB for GFDM demodulation bases while the $P_d$= 0.4390 at SNR = 8 dB and 0.6492 at SNR = 14 dB for OFDM demodulation bases. It is clear from the simulation results that the performance with GFDM outperformed OFDM. Lower out of band OOB emission due to flexibility selection of filter impulse response with GFDM compared with the OFDM, single CP is added to GFDM for *M*- sub-symbols, which causes better power and spectral efficiency.

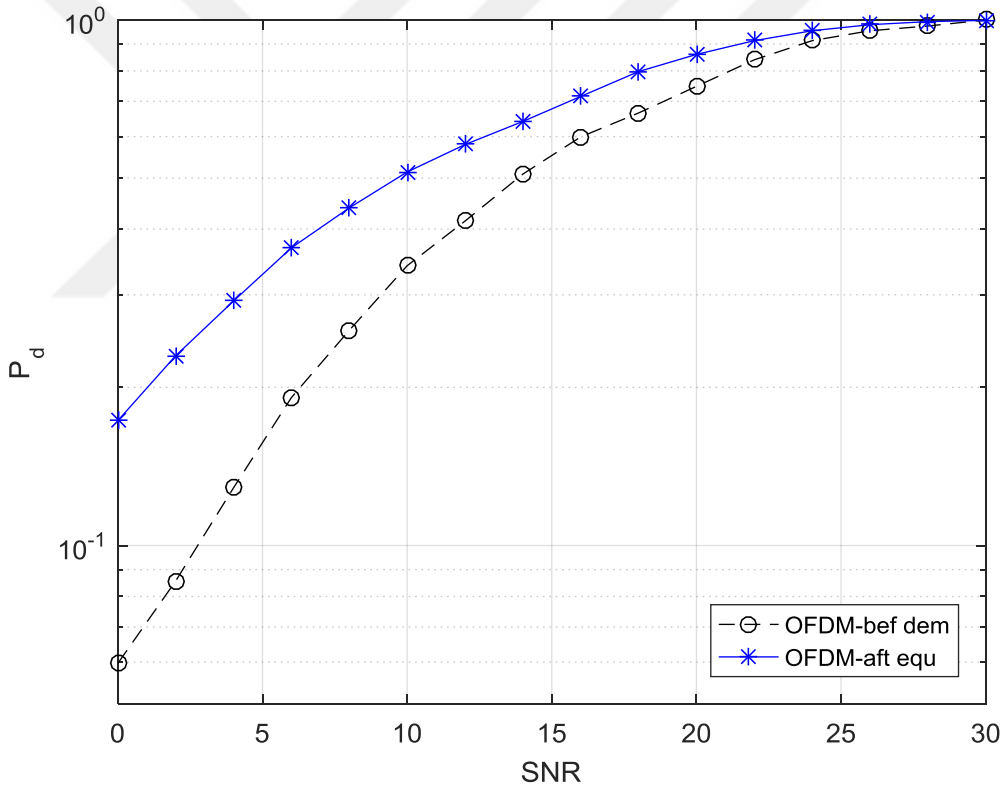


Figure 4.2 $P_d$ versus $SNR$ curves over Rayleigh fading channel before OFDM demodulation and after data equalization

Also, another simulation is done for comparison between sensing performance after data equalization for both GFDM and OFDM demodulation over Nakagami-$m$ ($m$ =3) fading channel is represented in Figure 4.4. The $P_d$ = 0.3797 at SNR = 4 dB with OFDM demodulation effects while reachs to 0.7041 under GFDM demodulation effect.

Hence, still the performance with the GFDM demodulation is better than with the OFDM due to the same above reasons.

In Fig. 4.5, a performance comparison in terms of $P_d$ for Rayleigh and Nakagami-$m$ fading channels (Rayleigh is a special case for Nakagami when $m$ =1) are drawn. In here, SNR from 0 dB to 30 dB values are used as boundary conditions, and the fading parameter $m$ is set to 1, 2, 3 respectively. This performance is studied in case of GFDM with implemented the channel estimation technique after the data equalization. From the figure, it is seen that the $P_d$ as expected, increases with increasing of SNR for both fading channels. For example as is given before the $P_d$ is equal to 0.532 at SNR = 6 dB and 0.8289 at SNR = 12 dB for fading parameter $m$ = 1 (Rayleigh fading). While the $P_d$ is equal to 0.6423 at SNR = 6 dB and 0.8529 at SRN = 12 dB for Nakagami parameter $m$ = 2 and for last, the $P_d$ is equal 0.8807 at SNR = 6 dB and 0.9994 at SNR = 12 dB for Nakagami parameter $m$ = 3. It is clear the best energy detection performance is when the fading parameter $m$ = 3, and lowest is when $m$ = 1, since the gain of the detection for Nakagami-$m$ fading is (t = $m$ -1) [76].

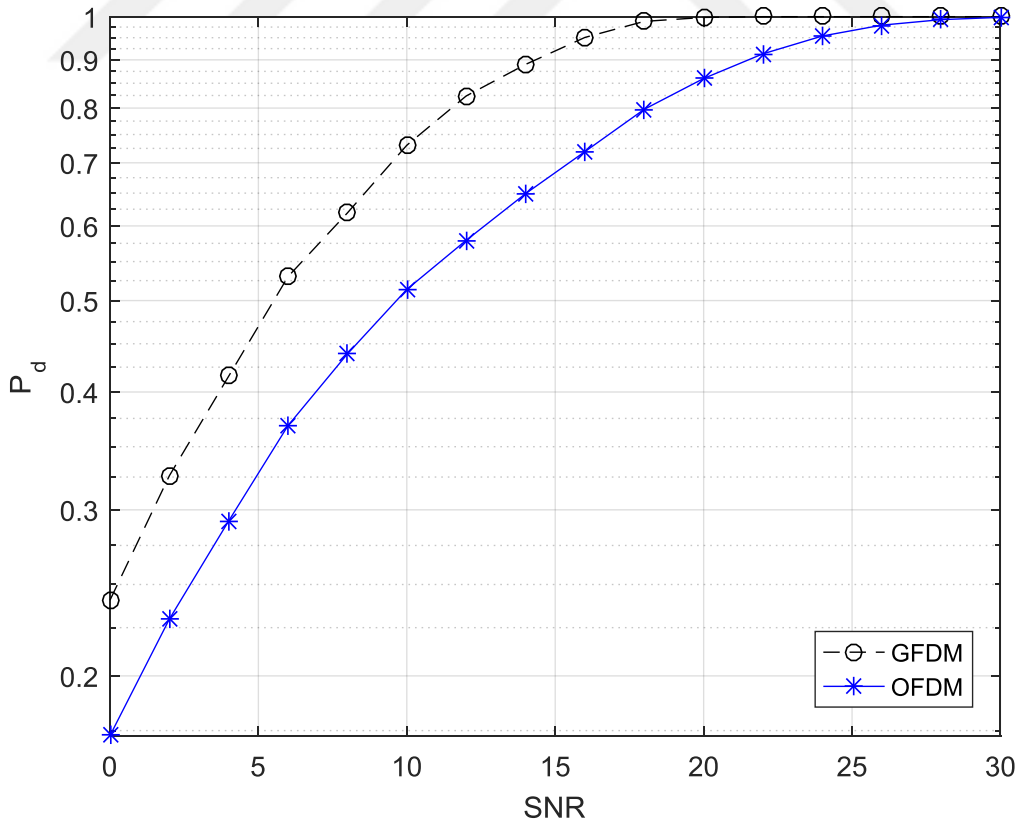


Figure 4.3 $P_d$ versus $SNR$ curves over Rayleigh fading channels for GFDM and OFDM after data equalization

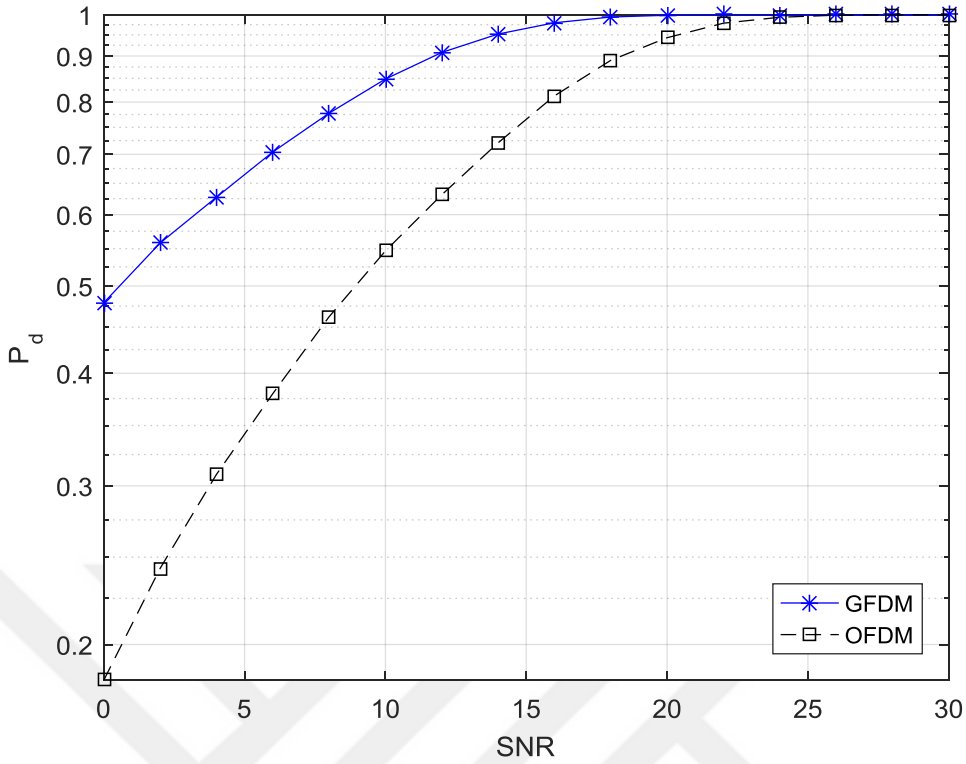


Figure 4.4 $P_d$ versus $SNR$ curves over Nakagami- $m$ ($m$ =3) fading channel for OFDM and GFDM after data equalization

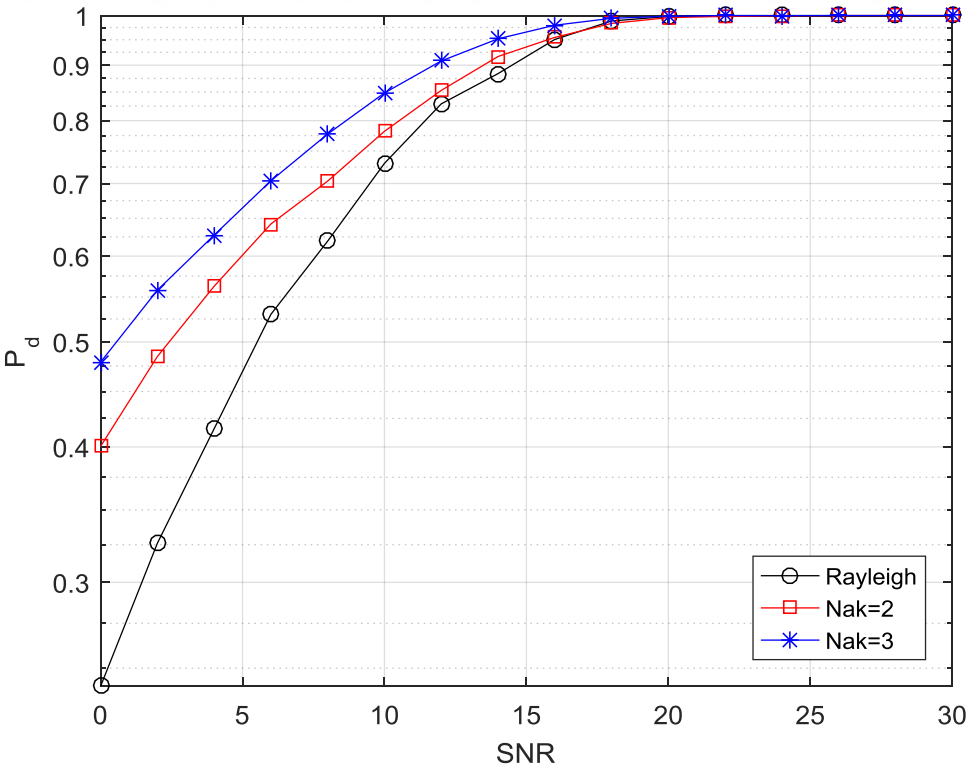


Figure 4.5 $P_d$ versus $SNR$ curves over fading channels after data equalization based GFDM

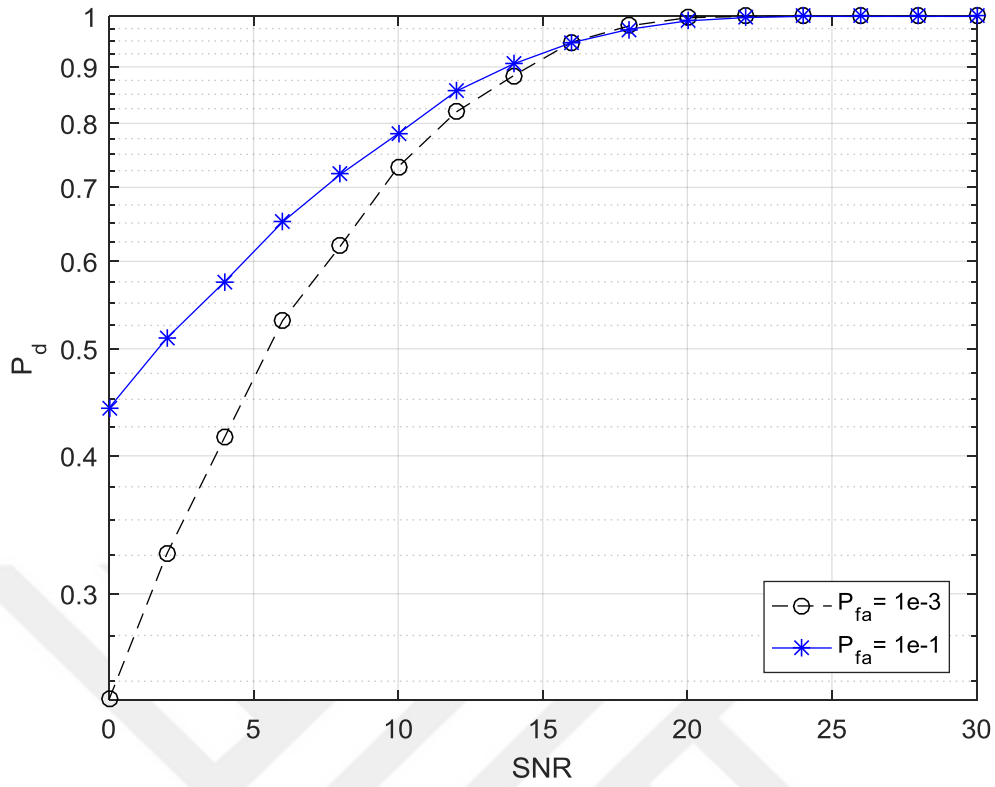


Figure 4.6 $P_d$ versus SNR for different $P_{fa}$ values over Rayleigh fading channel after data equalization based GFDM

ROC sensing performance analysis over Rayleigh fading channel in different $P_{fa}$ values for transceiver based on GFDM modulation is considered. The detection after the demodulation is investigated and illustrated as in Figure 4.6. This figure results show the effect of the required $P_{fa}$ on the $P_d$. It is clear from simulation results that the sensing performance increases for higher $P_{fa}$ and higher SNR. For example $P_d$ is equal to 0.532 at SNR=6 dB and 0.8289 at SNR=12 for $P_{fa} = 10^{-3}$ while equal to 0.6412 at SNR = 6 dB and 0.8554 at SNR = 12 dB for $P_{fa} = 10^{-1}$.

# CHAPTER 5

# CONCLUSION AND FUTURE WORK

## 5.1 Conclusion

The aim of this study is to analyze the spectrum sensing performance of energy detection technique based cognitive radio networks using a GFDM multicarrier physical layer. The sensing performance over Rayleigh and Nakagami-m fading channels are considered in this analysis. The obtained results can be summarized by

- the simulation results show that the detection performance for the opportunistic users increases with increasing SNR.
- the detection performance can be enhanced the energy detection is performed after the data equalization.
- the detection performance for transceiver using the GFDM multicarrier physical layer is better than with the OFDM.
- the simulation results show that the probability of detection increases when the fading parameter $m$ increases. The best detection gets in the case of higher Nakagami. This means that the higher value of the Nakagami fading parameter $m$, the better the detection performance. This supports the previous studies that are performed by [76] and [80].
- this study concludes that the transceivers bases GFDM multicarrier are more suitable for cognitive radio usage in terms of detection performance.

## 5.2 Future Work

Since the spectrum sensing is very important to improve the spectral efficiency, this helps to cover the increasingly demand for the frequency band. As a future work, spectrum sensing based cognitive radio performance may be improved by employing

cooperative systems. It is recommended to implement the cooperative system with the new proposed modulation GFDM for cognitive radio networks, then analyze and investigate the sensing performance of the proposed system model.

## REFERENCES


[1] Liang,Y.-C. Chen, K.-C. Li, G. Y. and Mahonen, P., (2011). "Cognitive radio networking and communications", IEEE Transaction Vehicular Technology, 60(7): 3386–3407.

[2] Niyato, D. Wang, P. and Kim, D. I., (2014). "Performance modeling and analysis T. of heterogeneous machine type communications", IEEE Transaction Wireless communication, 13(5): 2836-2849.

[3] Fettweis, G. P., (2014). "The tactile Internet: Applications and challenges" IEEE Vehicular Technology, 9(1): 64–70.

[4] Federal Communication Commission, FCC 03-322, 2003, Facilitating Opportunities for Flexible, Efficient, and Reliable Spectrum Use Employing Cognitive Radio Technologies, Washington, DC, USA.

[5] Haykin, S., (2005). "Cognitive radio: Brain-empowered wireless communications", IEEE Journal on Selected Areas in Communications, 23(2): 201–220.

[6] Q. Zhang et al., (2013). "On exploiting polarization for energy-harvesting enabled cooperative cognitive radio networking", IEEE Wireless Communication, 20(4):116–124.

[7] Federal Communications Commission, Tech. Rep. 04-113, 2004, Notice of proposed rule-making, in the matter of unlicensed operation in the TV broadcast bands and additional spectrum for unlicensed devices below 900 MHz and in the 3 GHz band, Washington, D.C.

[8] Federal Communications Commission, FCC 04-113, 2004, Notice of Proposed Rulemaking in the Matter of Unlicensed Operation in the TV Broadcast Bands (ET Docket No. 04-186) and Additional Spectrum for Unlicensed Devices Below 900 MHz and in the 3 GHz Band (ET Docket No. 02-380), Washington, D.C.

[9] Proakis, J. G., 2008, Digital communications, 5th Edition, Mc Graw-Hill, book Co., California USA.

[10] Gardner, W. A. Spoone, C. M., (1992). "Signal interception: performance advantages of cyclic-feature detectors", IEEE Transaction Communication, 40(1): 149-159.

[11] Taherpour, A. Gazor, S. Nasiri-Kenari, M., (2008). "Wideband spectrum sensing in unknown white Gaussian noise", IET Communications, 2(6):763-771.

[12] Yucek, T and Arslan, H., (2009). "A survey of spectrum sensing algorithms for cognitive radio applications", IEEE Communications Surveys Tutorials., 11(1): 116–130.

[13] Fettweis, G. Krondorf, M. and Bittner, S., (2009). "GFDM - Generalized Frequency Division Multiplexing", Vehicular Technology Conference,17-22 April 2009, Portogal.

[14] Datta, R. Fettweis, G. Koll´ar, Z. and Horv´ath P., (2011). "FBMC and GFDM Interference Cancellation Schemes for Flexible Digital Radio PHY Design", Euromicro Conference on Digital System Design, 31 Augest-2 September 2011, Finland.

[15] Datta, R. Michailow, N. Lentmaier, M. and Fettweis, G., (2012). "GFDM Interference Cancellation for Flexible Cognitive Radio PHY Design" ,Vehicular Technology Conference, 3-6 September 2012, Quebec City, QC, Canada.

[16] Michailow, N. Krone, S. Lentmaier, M. and Fettweis, G., (2012). "Bit Error Rate Performance of Generalized Frequency Division Multiplexing", Vehicular Technology Conference, 3-6 September 2012, Quebec City, QC, Canada.

[17] Bandari, S. K. Drosopoulos, A. Mani, V.V., (2015). "Exact SER Expressions of GFDM in Nakagami-m and Rician fading channels", European Wireless Conference, 20-22 May 2015, Hungary.

[18] Farhang, A. Marchetti, N., Doyle, L., (2015). "Low complexity GFDM receive design: a new approach", IEEE International Conference on Communications (ICC), 8-12 June 2015, London UK, 4775–4780.

[19] Gaspar, I. Michailow, N. Navarro, A. Ohlmer, E. Krone, S. and Fettweis, G., (2013). "Low Complexity GFDM Receiver Based on Sparse Frequency Domain Processing", Vehicular Technology Conference (VTC spring), 2013 IEEE 77th, 2-5 June 2013, New York, 1–6.

[20] Sumarsana, A. and Arseno, D., (2016). "Performance Analysis of Generalized Frequency Division Multiplexing in Various Pulse-shaping Filter for Next Generation Communication Systems", Asia Pacific Conference on Wireless and Mobile (APWiMob), 13-15 September 2016, Bandung – Indonesia, 41-45.

[21] Yenilmez, A. Gucluoglu, T. and Remlein, P., (2016). "Performance of GFDM-Maximal Ratio Transmission over Nakagami-m Fading Channels", International Symposium on Wireless Communication Systems ISWCS, 20-23 September 2016, Poland, 523-527.

[22] Mitola, J., 2000, Cognitive radio an integrated agent architecture for software defined radio, PhD Thesis, KTH Royal Institute of Technology, Stockholm Sweden.

[23] Rajbanshi, R., 2007, OFDM-based cognitive radio for DSA networks, Technical Report, The University of Kansas, Information & Telecommunication Technology Center, Kansas, USA.

[24] Maquire, G. Q. Jr., (2009). "Cognitive radio Making software radios more personal", IEEE Personal Communications, 6 (4):13-18.

[25] Mitola, J. and Hwu, J., (2010). Cognitive radio performance analysis and applications, PhD Thesis, State University of New York, New York, USA.

[26] Cabric, D. Mishra, S. M. and Brodersen, R. W., (2004). "Implementation Issues in Spectrum Sensing for Cognitive Radios", Proceeding 38th Asilomar Conference on Signals Systems and Computers, 7-10 November 2004, California. 772-776.

[27] Zhang, S. Zhang, H. and Zhu,L., (2012). "Multi-hop Diversity-Based Collaborative Spectrum Sensing in Cognitive Radio", Future Wireless Networks and Information Systems, 143:43–50.

[28] Haykin, S. Thomson, D. J., and Reed, J. H., (2009). "Spectrum sensing for cognitive radio", Proceedings of the IEEE, 97 (5): 849-877.

[29] Akyildiz, I., Lee, W. Y., Vuran, M. C., and Mohanty, S. (2008). "A survey on spectrum management in cognitive radio networks", IEEE Communications Magazine, 46(4):154-160.

[30] İlhan, H., (2011). Cooperative system design and error performance analysis for Cascade damped channels, Doctorate Thesis, Istanbul Technical University, Institute of Science, Istanbul.

[31] Michailow, N. Lentmaier, M. Rost, P. and Fettweis, G., (2011). "Integration of a GFDM Secondary System in an OFDM Primary System", Future Network Summit, 15-17 June 2011, Poland.

[32] Datta, R. Panaitopol, D. and Fettweis, G., (2012). "Analysis of Cyclostationary GFDM Signal Properties in Flexible Cognitive Radio," in Communications and Information Technologies (ISCIT), International Symposium, 2-5 October 2012, Australia, 663–667.

[33] Panaitopol, D. Datta, R. and Fettweis, G., (2012). "Cyclostationary Detection of Cognitive Radio Systems Using GFDM Modulation", Wireless Communications and Networking Conference (WCNC), 1-4 April 2012, China.

[34] Datta, R. Arshad, K. and Fettweis, G., (2012). "Analysis of Spectrum Sensing Characteristics for Cognitive Radio GFDM Signal", International Wireless Communication and Mobile computing Conference (IWCMC), 27-31 August 2012, Cyprus.

[35] Yucek, T. and Arslan, H., (2009). "A Survey of Spectrum Sensing Algorithms for Cognitive Radio Applications", IEEE Communications Surveys & Tutorials, 11(1):116–130.

[36] Hwang, C.-H. Lai, G.-L. and Chen, S.-C., (2010). "Spectrum Sensing in Wideband OFDM Cognitive Radios", IEEE Transactions on Signal Processing, 58: 709 –719.

[37] Wylie-Green, M., (2005). "Dynamic spectrum sensing by multiband OFDM radio for interference mitigation", New Frontiers in Dynamic Spectrum Access Networks on International Symposium, 2005. 8-11 November 2005, Baltimore USA, 619 –625.

[38] Datta, R. Michailow, N. Krone, S. Lentmaier, M. and Fettweis, G., (2012). "Generalized Frequency Division Multiplexing in Cognitive Radio", 20th European Signal Processing Conference (EUSIPCO), 27-31 August 2012, Romania, 2679–2683.

[39] TSE 9792, (2005). Fundamentals of Wireless Communication, TSE, Cambridge University Press.

[40] Nicola M., (2015). Generalized Frequency Division Multiplexing Transceiver Principles, PHD. Thesis, der Fakultät Elektrotechnik und Informations technik der Technischen Universität Dresden, zurErlangung des akademischen Grades eines, Germany.

[41] Theodore S. Rappaport, (1999). Wireless Communications: principles and practice, Illustrated edition, English, Book, Upper Saddle River, N.J., Prentice Hall PTR.

[42] Simon M.K. and, Alouini, M.S., (2000). Digital Communications over Fading Channels: A Unified Approach to Performance Analysis, 6th ed., John Wiley & Sons Inc., New York.

[43] Naguib, A. F. Tarokh, V. Seshadri, N. and Calderbank, A. R., (1998). "A space-time coding modem for high-data-rate wireless communications", IEEE Journal on Selected Areas Communication, 16:1459–1478.

[44] Tarokh, V. Naguib, A. F. Seshadri, N. and Calderbank, A. R., (1999). "Space-time codes for high data rate wireless communication: Performance criteria in the presence of channel estimation errors, mobility, and multiple paths", IEEE Transaction Communication, 47:199–207.

[45] RT. Ministry of Environment and Forest General Directorate of Forestry, Main Tree Species, www.ogm.gov.tr/agaclar.htm, 11 March 2012.

[46] Nakagami, M., (1960). "The m-distribution: A general formula of intensity distribution of rapid fading", Statistical Methods in Radio Wave Propagation, 10: 3–36.

[47] Mosier, R. and Clabaugh, R., (1958). "A bandwidth-efficient binary transmission system", American Institute of Electrical Engineers Part I: Communication and Electronics Transactions, 76(6):723–728.

[48] Saltzberg, B., (1967). "Performance of an Efficient Parallel Data Transmission System", Communication Technology IEEE Transactions, 15(6):805–811.

[49] Chang, R. W., (1966). "Synthesis of Band-Limited Orthogonal Signals for Multichannel Data Transmission", The Bell Systems Technical Journal, 45(10):1775–1796.

[50] Bingham, J. A., (1990). " Multicarrier modulation for data transmission: An idea whose time has come", Communications Magazine, IEEE, 28(5):5–14.

[51] Mirahmadi, M. Al-Dweik, A. and Shami, A., (2013). "BER Reduction of OFDM Based Broadband Communication Systems over Multipath Channels with Impulsive Noise", IEEE Transactions on Communications,61(11):4602–4615.

[52] Dinur, N. and Wulich, D., (2001). "Peak-to-average power ratio in high-order OFDM Communications", IEEE Transactions, 49(6):1063–1072.

[53] Wunder, G. et al., (2014). "5G NOW: non-orthogonal, asynchronous waveforms for future mobile applications", IEEE Communications Magazine, 52(2):97–105.

[54] ITU-R BT.1206-2, (2014). Spectrum limit masks for digital terrestrial television broadcasting.

[55] Bellanger. M. 2010, FBMC physical layer a primer, PHYDYAS Technical report, Canada.

[56] Doré, J.-B. Berg, V. Cassiau, N. and Kténas, D., (2014). "FBMC receiver for multi-user asynchronous transmission on fragmented spectrum", EURASIP Journal on Advances in Signal Processing, 201: 21–20.

[57] Kanaras, I. Chorti, A. Rodrigues, M. R. and Darwazeh. I., (2009). "Spectrally efficient FDM signals: bandwidth gain at the expense of receiver complexity", ICC'09. IEEE International Conference, 14-18 June 2009, Dresden Germany, 1–6.

[58] Anderson, J. B. Rusek, F. and Owall, V., (2013). "Faster-than-Nyquist signaling", Proceedings of the IEEE, 101(8):1817–1830.

[59] Liveris, A. D. and Georghiades, C. N., (2003). "Exploiting faster-than-Nyquist signaling", Communications IEEE Transactions, 51(9):1502–1511.

[60] Vakilian,V. Wild,T. Schaich, F. ten Brink, S. and Frigon J.-F., (2013). " Universal- filtered multi-carrier technique for wireless systems beyond LTE", Globecom Workshops (GC Wkshps), 9-13 December 2013, Atlanta USA.

[61] Matthé, M. Michailow, N. Gaspar, I. and Fettweis, G., (2014). "Influence of Pulse Shaping on Bit Error Rate Performance and Out of Band Radiation of Generalized Frequency Division Multiplexing", IEEE International Conference Communication Workshop (ICC), 10-14 June 2014, Sydney Australia, 43-48.

[62] Heideman, M. T. Johnson, D. H. and Burrus, C. S., (1984). "Gauss and the history of the fast Fourier transform", ASSP Magazine IEEE, 1(4):14–21.

[63] Nee R. v. and Prasad, R. (2000). OFDM for wireless multimedia communications, First Edition, Artech House, USA.

[64] Batra, A. Balakrishnan, J. and Robert Aiello, G. (2004). "Multiband OFDM UWB System in the Presence of Log-normal Fading Channels", 52(9):2123-2138.

[65] Khan, R. Altunbas, I. Kurt, G. K. (2016). "Channel Coded Complex Field Network Coding with OFDM in Wireless Networks" Advance in Wireless and Optical Communication (RTUWO), 3-4 November 2016, Riga, Latvia.

[66] Georgia, D. Ntouni, M. and George, K., (2017). "On the Optimal Tone Spacing for Interference Mitigation in OFDM-IM Systems", IEEE Communications Letters, 21(5):1019-1022.

[67] Hunt, B., (1972). "A matrix theory proof of the discrete convolution theorem", IEEE Transactions on Audio and Electro acoustics, 19(4):285–288.

[68] Ivan S., (2016). Waveform Advancements and Synchronization Techniques for Generalized Frequency Division Multiplexing, PHD. Thesis, der Fakultät Elektrotechnik und Informations technik der Technischen Universität, zur Erlangung des akademischen Grades eines.

[69] Farhang-Boroujeny, B., (2011). "OFDM versus Filter Bank Multicarrier", IEEE Signal Processing Magazine, 28(3):92–112

[70] Le Floch, B. Alard, M. and Berrou, C., (1995). "Coded orthogonal frequency division multiplex [TV broadcasting]", Proceedings of the IEEE, 83(6):982–996.

[71] Hidalgo Stitz, T. Ihalainen, A. Viholainen, and M. Renfors "Pilot Based Synchronization and Equalization in Filter Bank Multicarrier Communications," EURASIP Journal on Advances in Signal Processing, May 2010.

[72] Michailow, N. Matthe, M. Gaspar, I. Caldevilla, A. Mendes, L. Festag, A. and Fettweis, G., (2014). "Generalized Frequency Division Multiplexing for 5th generation cellular networks", Communications IEEE Transactions, 62(9):3045–3061.

[73] Bandari, S. K. Vakamulla, V. M. and Drosopoulos, A., (2017). "Training Based Channel Estimation for Multitaper GFDM System", Hindawi Mobile Information Systems, 17: 8-16.

[74] Cai, X. and Georgios Giannakis, B., (2004). "Error Probability Minimizing Pilots for OFDM With M-PSK Modulation Over Rayleigh-Fading Channels", IEEE Transactions on vehicular technology, 53(1):146-155.

[75] Atapattu, S. Tellambura, C. Jiang, H., (2014). Energy Detection for Spectrum Sensing in Cognitive Radio, New York.

[76] Quan, Z. Cui, S. Sayed, A. H. H. Poor, V., (2009). "Optimal multiband joint detection for spectrum sensing in cognitive radio networks", IEEE Ton Signal Processing, 57(3):1128–1140.

[77] Cabric, D. Artem, T.o and Brodersen R. W., (2018). "Experimental Study of Spectrum Sensing based on Energy Detection and Network Cooperation", Berkeley Wireless Research Center, 9(7):321-325.

[78] Alghamdi, O. A. Ahmed M. Z. and Abu-Rgheff, M. A., (2010). "Probabilities of Detection and False Alarm in Multitaper Based Spectrum Sensing for Cognitive Radio Systems in AWGN", IEEE International Conference on Communication Systems, 17-19 November 2010, Singapore, 579 – 584.

[79] Digham, F. F. Alouini, M. S. and Simon, M. K., (2007). "On the energy detection of unknown signals over fading channels", IEEE Transaction Communication, 55(1):21–24.

## CURRICULUM VITAE

### PERSONAL INFORMATION


**Name Surname** : Nidaa AL-HASAANI

**Date of birth and place** : 05/09/1972- Iraq Baghdad

**Foreign Languages** : English, Turkish

**E-mail** : engnidaa72@gmail.com


### EDUCATION

| Degree | Department | University | Date of Graduation |
|---|---|---|---|
| Master | | | |
| Undergraduate | Electrical engineering | Baghdad University/Iraq | 1995 |
| High School | Al Hurryia School | | 1990 |

### WORK EXPERIENCE

| Year | Corporation/Institute | Enrollment |
|---|---|---|
| 2009 | Ministry of communication | Project manager |
| 2006 | Zain- Iraq for mobile network | Core optimization manager |

| | | |
|---|---|---|
| 1996 | Ministry of communication | Project manager |

**PUBLISHMENTS**

**Papers**

1. Spectrum Sensing Performance for Cognitive Radio networks with GFDM Modulation over Nakagami-*m* Channel.

**Conference Papers**

1. Energy Detection of Spectrum Sensing for Cognitive Radio Networks Using GFDM Modulation.